Performance Analysis of the Power Splitting Simultaneous Lightwave Information and Power Transfer (PS-SLIPT) Architecture

Sumali Saumya Morapitiya

(188111E)

Thesis submitted in partial fulfillment of the requirements for the degree
Master of Philosophy

Department of Electronic and Telecommunication Engineering

University of Moratuwa
Sri Lanka

December 2021

Declaration

I declare that this is my own research proposal and this proposal does not incorporate without acknowledgement any material previously published submitted for a Degree or Diploma in any other university or institute of higher learning and to the best of my knowledge and belief, it does not contain any material previously published or written by another person except where the acknowledgement is made in the text.

Signature of the Student:..... *Date:.....*

I have read the proposal and it is in accordance with the approved university proposal outline. I am willing to supervise the research work of the above candidate in the proposed area.

Signature of the Supervisor:..... *Date:.....*

Prof. Dushantha Nalin K.Jayakody, Sri Lanka Technological Campus (SLTC), Sri Lanka.

Signature of the Supervisor:..... *Date:.....*

Prof. L.W.P. R Udayanga, University of Moratuwa, Sri Lanka.

Abstract

Recent studies done on Simultaneous Lightwave Information and Power Transfer (SLIPT) has become a hot topic among the research community. The importance of the SLIPT is to harvest energy using light sources while decoding the information. In this thesis work, we present the mathematical framework for the Power Splitting (PS) based SLIPT system and study the performance of the PS-SLIPT and Time Splitting (TS)-SLIPT architectures. Moreover, we quantitatively study the harvested energy with different Field of View (FoV) angles of the Light Emitting Diode (LED) and the Photodiode (PD). In addition, analyze the important parameter of the Visible Light Communication (VLC) system to achieve maximum received power and we consider the amount of harvested energy for different Direct Current (DC) values. Overall, concludes that the Field of View (FoV) and DC bias signals are directly affected by SLIPT systems. Using numerical simulations, we demonstrate the performance of the both architectures to enhance the QoS of information decoding data rate, amount of harvested energy and trustworthiness of the information.
Further, our research work extend to Simultaneous Wireless Information and Power Transfer (SWIPT) technique is introduced in Radio Frequency (RF) communication to carry both information and power in same medium. In this approach, the energy can be harvested while decoding the information carries in an RF wave. Recently, the same concept apply in VLC namely SLIPT, which is highly recommended in an indoor applications to overcome the problem facing in RF communication. Thus, the SLIPT is introduce to transmit the power through a Light Emitting Diode (LED) luminaries. In this work, we compare both SWIPT and SLIPT technologies and realize SLIPT technology archives increase performance in terms of the amount of harvested energy, outage probability and error rate performance.

Index terms - Outage Probability, Simultaneous Lightwave Information and Power Transfer (SLIPT), Simultaneous Wireless Information and Power Transfer (SWIPT), Visible Light Communication (VLC), Energy Harvesting (EH), Light Emitting Diode (LED), Information Decoding (ID)

List of publications

1. **Sumali S. Morapitiya**, Mohammad Furqan Ali, Samikkannu Rajkumar, Sanika K. Wijayasekara, Dushantha Nalin K. Jayakody and R.U.Weerasuriya "A SLIPT-Assisted Visible Light Communication Scheme" *IEEE International Conference on Distributed Computing in Sensor System (DCOSS)*, California, USA, 15^{th} June 2020.

2. **Sumali S. Morapitiya**, TWW Leelarathna, Dushantha Nalin K. Jayakody and RU Weerasuriya "Performance Analysis of the SLIPT Architectures" *10th IEEE International Conference on Information and Automation for Sustainability 2021 (IEEE ICIAFS 2021)*, Sri Lanka, 15^{th} August 2021.

Acknowledgements

I would like to extend my gratitude to my supervisors, Prof. L.W.P. Ruwan Udayanga, Department of Electronic and Telecommunication Engineering, University of Moratuwa and Prof. Dushantha Nalin K. Jayakody, Head - School of Postgraduate Research, Sri Lanka Technological Campus (SLTC), Padukka, Sri Lanka and professor at the School of Computer Science & Robotics, National Research Tomsk Polytechnic University (TPU), Russia for their academic advice, continuous guidance and the tremendous support given to me throughout my research study. I am extremely grateful that you took me on as a student and continued to have faith in me over the years.

I am fortunate to have been a part of the Center for Telecommunication Research (CTR) committee member - SLTC. Your encouraging words and thoughtful, detailed feedback have been very important to me. My appreciation also goes out to my family and friends for their encouragement and support all through my studies.

Contents

List of Figures

List of Tables

List of Abbreviations

Abbreviation	Description
AC	Alternative Current
AF	Amplify and Forward
APD	Avalanche Photo Diode
AWGN	Additive White Gaussian Noise
BER	Bit Error Rate
CSK	Colour Shift keying
DC	Direct Current
DCN	Data Center Network
DF	Decode and Forward
dLoS	direct Line of Sight
DPSK	Differential Phase Shift keying
EH	Energy Harvesting
FCC	Federal Communication Commission
FF	Fill Factor
FoV	Field of View
FPGA	Field Programmable Gate Array
FSO	Free Space Optics
ID	Information Decoding
IM/DD	Intensity Modulation/Direct Detection
IoT	Internet of Things
IR	Infrared
LAN	Local Area Network
LED	Light Emitting Diode
LoS	Line of Sight
OWC	Optical Wireless Communication
MAN	Metropolitan Area Network
MIMO	Multiple Input Multiple Output

MSN	Minimum Shift Keying
NRZ	Non-Return Zero
OFDM	Orthogonal Frequency Division Multiplexing
OLED	Organic LED
OOK	On-Off Keying
PD	Photo-diode
PPM	Pulse Position Modulation
PWM	Pulse Width Modulation
PS	Power Splitting
QoS	Quality of Service
RAT	Relay Assisted Technology
RF	Radio Frequency
SLIPT	Simultaneous Lightwave Information and Power Transfer
SPPM	Spatial Pulse Position Modulation
SSK	pace-Shift-Keying
SNR	Signal to Noise Ratio
SPAD	Single Photon Avalanche Diode
SWIPT	Simultaneous Wireless Information and Power Transfer
TDMA	Time Division Multiple Access
TS	Time Splitting
UV	Ultra Violet
UWAV	Underwater Autonomous Vehicle
VLC	Visible Light Communication
VPPM	Variable Pulse Position Modulation
V-to-V	Vehicle to Vehicle
WHO	World Health Organization

Chapter 1

INTRODUCTION

Energy Harvesting is the process by which energy is derived from external sources. The growth and development of the future communication industry faced high energy consumption of wireless networks as a challenge. Energy harvesting is an ideal solution for low power device enabled networks such as sensor networks and the Internet of Things (IoT) to offer a reliable solution [6].

1.1 Optical Wireless Communication (OWC)

Due to the rapid increase in the wireless capacity for high data rates and multimedia applications, the wireless communication field is facing a lot of difficulties at present. The existing microwave RF communication range is not at a satisfactory level to overcome this issue. However, OWC has an unregulated spectrum with high bandwidth and it provides a solution for ongoing crisis. Also, it is used for indoor and outdoor applications and multimedia applications [7]. There are some significant property differences in both systems. In RF communication it operates under a regulated bandwidth, pass through the object, multi-path fading, multi-path propagation. Further, the VLC is on unregulated bandwidth, cannot pass through the object or wall, no multi-path fading, no multi-path propagation. However, both technologies have high path loss [8]. The optical communication range is from 300GHz to 3000THz. The Free Space Optics (FSO) is used for unguided data transmission using optical carriers such as Ultra Violet (UV), Infrared (IR) and Visible Light. The FSO communication system gives more beneficial than RF communication such as high rate communication, high optical bandwidth, use of tiny laser beams, provide high security and robustness of the signal. There are several applications introduced in FSO communication. The university network connections, surveillance monitoring, cellular communications, disaster monitoring, security applications and broadcasting. [9].

In this Chapter, we discuss the VLC and it is a subset of the OWC. Also, we introduce the novel topic SLIPT and it is the subset of VLC. Figure 1.1 shows in

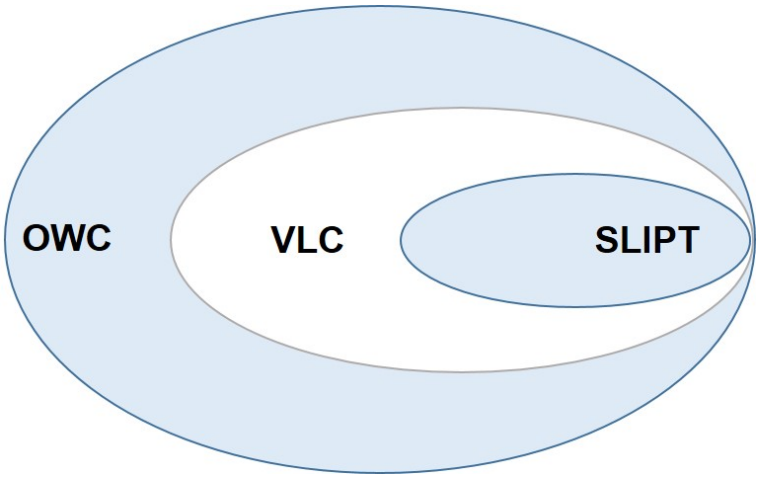

Figure 1.1: The SLIPT relate with existing technologies.

the SLIPT relate with existing technologies.

1.2 Visible Light Communication (VLC)

Visible Light Communication (VLC) is a new technology in OWC . It is introduced the year 2000 [10]. VLC delivers high-speed wireless communication in day to day life. There are limitations of the Radio Frequency (RF) technology and to conquer the restraint of RF, introduce the VLC technology. This is comparatively inexpensive, has high security, high bandwidth, low energy consumption and can use existing light infrastructure [11].

VLC communication fulfils two areas: illumination and communication. VLC is a wireless transmission method and it uses a wavelength range from 380nm to 750nm (frequency range from 430THz to 790THz) for communications. This is short-range communication technology and uses for three main areas: indoor communications, outdoor communications and underwater communications. There are some salient features of VLC technology such as bandwidth, efficiency, availability, reliability, speed, capacity and security [12]. In VLC technology, the LED is used as a transmitter and it has a low thermal resistance and can emit high optical power. LEDs are generally used for two purposes: illumination and communications. High luminous efficiency, small size and long lifetime are the advantages of the LED. Current and junction temperature are the factors affecting the light output of the LED. When the current increase, the light output of the LED also increases. At the same time forward voltage and power dissipation increase. Similarly, temperature increases and efficiency and light output also decrease. Photo-diode uses as a receiver and Single Photon Avalanche Diode (SPAD) and

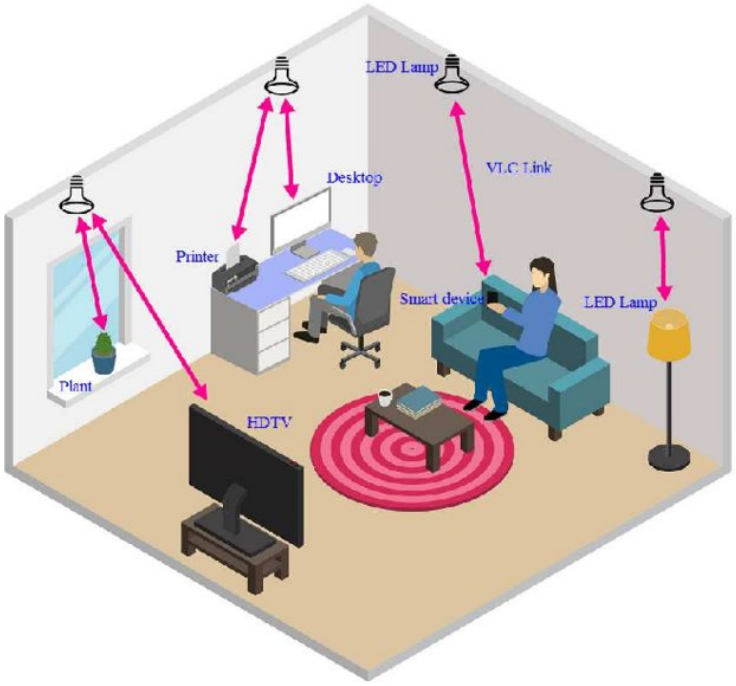

Figure 1.2: Basic concept of VLC [1].

Avalanche Photo Diode (APD) and can be used to optimize the receiver in VLC. Several factors affect the received signal, such as multi-path scenario, the distance between transmitter and receiver, receiver noise (shot and thermal), external sources (noise), Lambertian influence, dimming (sleeping mode, reading mode, normal mode) and the number of sources [13]. FoV of transmitter and receiver is the prime parameter that considers the Line-of-Sight (LoS) between the transmitter and the receiver in VLC [2].

Also, VLC completed three goals of future communication such as high-speed data rate, energy-efficient, and sustainable wireless communication [14]. Figure 1.2 shows the gaining knowledge about the basic concept of VLC communication and how it applies in an indoor communication system.

1.3 Simultaneous Lightwave Information and Power Transfer (SLIPT)

The SLIPT introduces EH, in addition to legacy simultaneously illumination and communication. [15]. In recently proposed SLIPT system, it divides the received

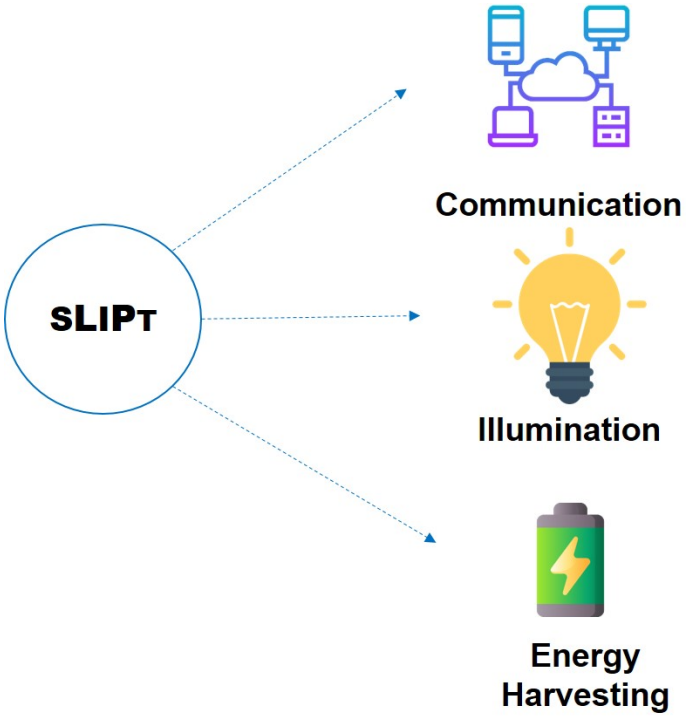

Figure 1.3: The basic SLIPT functions.

photon current into two parts as Alternative Current (AC) and DC to ID and EH respectively. In the SLIPT scheme, separated DC used to be stored in the battery for backup power and the remaining power is used to detect the information. The solar cell converts the optical signal into an electric signal and it is a reliable option to design the SLIPT receiver [16].

1.4 SLIPT Receiver Architectures

In general, mainly two receiver architectures are introduced in the SLIPT scenario such as PS-SLIPT receiver architecture and TS-SLIPT receiver architecture [17]. The importance of the receiver design is to separate the receiver signal in two different functions namely ID and EH. These systems use solar cell-based receiver architectures and work on power and time domain [2]. Figure 1.3 shows the basic functions of the SLIPT concept. Figure 1.4 shows the SLIPT receiver architectures and (a) shows the TS-SLIPT receiver architecture and (b) shows

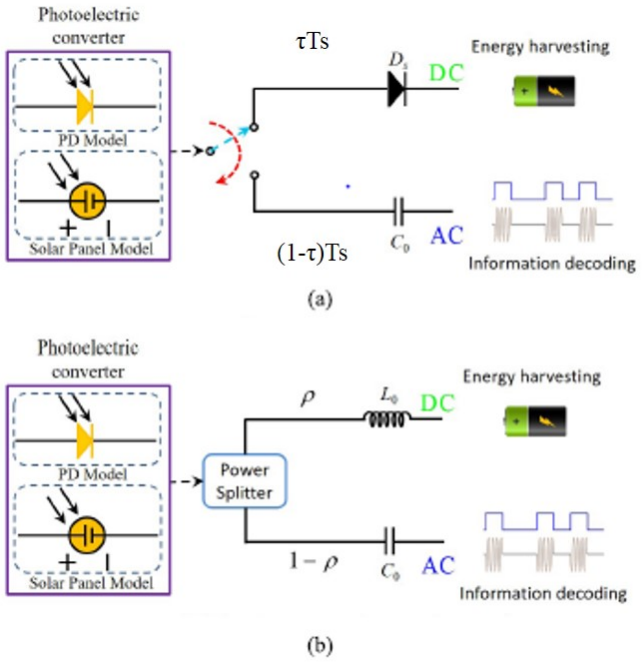

Figure 1.4: (a) TS receiver architecture. (b) PS receiver architecture [2].

the PS-SLIPT receiver architecture.

1.4.1 Power Splitting SLIPT Architecture (PS-SLIPT)

The PS receiver divides the received signal into two power streams. Afterwards, both power streams are sent to an information decoder and energy harvester to make possible simultaneous ID and EH. Apart from the receiver circuit, no additional change is required in the power-splitting design of conventional communication systems. In each receiver the PS ratio can be optimized. Furthermore, by varying PS ratios, the information rate and the harvested energy can be balanced according to the system requirements. Overall performance also can be improved by optimizing the combination of the signal and the PS ratios. Let ρ denotes the power-splitting coefficient value for EH and (1-ρ) for the ID [18].

1.4.2 Time Splitting SLIPT Architecture (TS-SLIPT)

The receiver used in this architecture contains an energy harvester, information decoder and a switch to change the time allocation in the system. Based on a TS sequence, the receiver change between ID and EH circuit periodically. Further-

more, the TS receiver also requires accurate information/energy scheduling and time synchronization. T is the time splitting coefficient and the range is [0,1]. The τT_s time slot used for the EH and $(1-\tau)T_s$ used for ID [19]- [20].

1.5 Simultaneous Wireless Information and Power Transfer (SWIPT)

The SWIPT is one of the EH technology in the wireless communication field and it is based on RF wireless communication. There are two methods EH from SWIPT such as ambient signal and base station source power. The applications depend on two categories as near-field and far-field. Recently, transmitters and receivers are more efficient and sizes are smaller. There are several advantages identified in the SWIPT system namely, power and spectral efficiency and control of the interference. The free space is the channel to transmit RF energy for their applications [17], [21].

1.6 Contribution

We explore the performance analysis of the PS-SLIPT architecture. There are four objectives defined for the research. There are

- To improve the energy harvesting by exploring power splitting receiver architecture.
- To study the impact of the system performance parameter such as Signal to Noise Ratio (SNR) and Bit Error Rate (BER).
- To study the different modulation schemes for PS-SLIPT architecture.
- To design the optimal receiver for the SLIPT architecture to guarantee an acceptable information rate and energy harvesting rate.

The contributions of this thesis are summarized as follows.

- We study the VLC communication system and compare it with RF communication. Further, comprehensive analysis of the benefits of using VLC for data transmission over radio and microwave frequency spectrum. We study the main parts of VLC technology such as a transmitter, receiver and channel. Furthermore, we simulate the channel model using Lambertian model in direct LoS (dLoS) in a VLC free space channel.

- We study the system model of the VLC and identify the important parameters. Also, we observe the behaviour of the received power when changing the parameters such as FoV of the transmitter and the receiver and distance between the transmitter and the receiver. Then, we select the FoV that gives the maximum received power.

- We explore research in the main areas of SLIPT technology and consider indoor communication in SLIPT and SWIPT. Also, we observe the behaviour of BER and SNR of both system models. Moreover, we study the outage probability and amount of energy harvesting of both system models.

- The research focus on SLIPT strategies such as adjusting the channel between the transmitter and the receiver, changing the transmission and changing the reception. Also, we study the performance analysis of power splitting SLIPT architecture and analyze the behaviour of the BER, SNR, ID rate and amount of harvested energy to maintain the QoS of the system. Finally, we study the SLIPT receiver architecture such as PS and TS and perform analysis of the PS and TS SLIPT architectures.

1.7 Outline of the Thesis

The organization of the chapters is as follows:

- Chapter 1: Introduction
  This chapter presents the background knowledge about OWC, VLC, SLIPT system, SLIPT architectures (PS and TS), SWIPT and an overview about the work carried out including its scope.

- Chapter 2: Literature Review
  This chapter summarizes the related research conducted and different techniques used in VLC and PS SLIPT architecture.

- Chapter 3: System Model
  This chapter includes, VLC system model, mathematical model for the VLC transmitter, mathematical model for the free space channel, mathematical model for the receiver, SLIPT receiver architectures, received electrical signal, AC component of the received signal $i(t)$ - ID, DC component

of the received signal I_{DC} - EH, a SLIPT-assisted visible light communication scheme, SWIPT system model: SM-I, RF-energy harvesting in SWIPT protocol, outage probability analysis for SM-I, SLIPT system model: SM-II and outage probability analysis for SM-II.

- Chapter 4: Results and Discussion
  This chapter presents the results obtained and analyzes the performance. Performance analysis of the SLIPT architectures, optimal FoV angle of Tx and Rx, BER analysis in PS-SLIPT architecture using different modulation schemes, behaviour of the ID data rate vs splitting coefficient in PS and TS SLIPT architectures, observe the behaviour of the energy harvesting vs splitting coefficient in PS and TS-SLIPT architectures,observe the behaviour of the EH vs ID in PS and TS-SLIPT architectures for different bias values, sub optimal splitting coefficient with BER in PS and TS-SLIPT architectures under Additive White Gaussian Noise (AWGN), calculate the amount of harvested energy for optimal splitting coefficient and assume threshold SNR, analyze the PS and TS-SLIPT architecture in EH and ID, a SLIPT-assisted visible light communication scheme, BER analysis of the SWIPT and SLIPT, outage probability analysis of the SWIPT and SLIPT, amount of harvested energy in SWIPT and SLIPT.

- Chapter 5: Conclusion
  This presents the conclusion of the proposed system model.

- Chapter 6: Future Directions
  This chapter describes future improvements that could be used to improve further.

Chapter 2

LITERATURE REVIEW

In this chapter, we present the background study of the existing technology of the OWC, FSO, VLC and SLIPT systems. First, we collect the information of the OWC and FSO to relate with VLC. After we gather the information about the basic literature of application and advantages of the VLC. Then, we focus on the VLC transmitters, VLC receivers and channel model of VLC. Also, discuss the existing modulation techniques use in VLC and how to apply them. Further, we focus on the EH, SLIPT and SWIPT system models. Finally, we pay the attention to the limitations of the VLC.

2.1 Optical Wireless Communication (OWC) / Free Space Optics (FSO)

The OWC is the promising technology than RF technology in our day to day life. For future IoT applications need high data rates and OWC is the most comfortable solution for the wireless communication industry. Also, OWC is a suitable answer for the fifth-generation wireless communication systems. In [22], introduced the two-hybrid communication system such as RF/optical hybrid communication and optical/optical hybrid system. Moreover, both systems help to overcome the limitations of both technologies and denote high performance for wireless communication. Also, increased reliability of the systems, successful achievable data rate and efficiency. In [23], discussed the relay systems for wireless communication. There are two methods in cooperative communication such as Amplify and Forward (AF) and Decode and Forward (DF) to apply for the relay system. Here, discussed the importance of the relay system and it helps to communicate for long-distance communications. When using the large distance communication we came across atmospheric turbulence, obstacle and weather condition. Therefore, Relay Assisted Technology (RAT) was introduced for indoor, outdoor and underwater applications.
In [24], presented FSO channel models such as misalignment losses with geometric

influence, environment affected noises and background noises and radiation. Also, discussed transceiver models and structures. Further, it is discussed RF/FSO hybrid models, cooperative communications and adaptive transmission. In [25], discussed apply FSO for Data Center Network (DCN). Most of the DCN work on the wired network. However, it is faced many difficulties such as cabling complexity. Therefore, introduced FSO link communication to overcome this issue. In [10], analyzed the BER, Q-factor and receiver sensitivity of the FSO communication. Further, it is used Minimum-Shift Keying (MSK) and Differential-Phase-Shift Keying (DPSK). However, DPSK has shown a better BER performance than MSK. There are five categories such as availability of LoS, length of the link, coverage area, environment and mobility are introduced in [26] for the FSO communication. Also, consider the link LoS or nLoS and fixed or mobile. Further, it is discussed the behaviour of five categories when applying the four types of environments namely indoor, terrestrial, space and underwater. In [9] FSO extended to application for the Metropolitan Area Network (MAN), Local Area Network (LAN)-to-LAN connectivity and video communication. In [26], investigated the internal parameters of the FSO system to optimize maximum output and the throughput of the communication. The parameters are wavelength and beam divergence. Further, the system model has used PIN diode and avalanche photodiodes and also compared both photodiodes. In [10], investigated the internal parameters of the FSO system to optimize maximum output and the throughput of the communication. The parameters are wavelength and beam divergence. Further, the system model has used PIN diode and avalanche photodiodes and also compared both photodiodes. Transmission power, the variance of the transmitted beam, receiver aperture, sensitivity of the receiver, optical loss are the parameters which depend the performance of the FSO system [27].
In [28], discussed the indoor and outdoor communication using FSO for 30m and 12m respectively. Also, compared the between RF and IR. Further, discussed the pros and cons of the both technologies. In [29], explained the factors affected to Q-factor in FSO communication. Transmit power, type of detection, modulation types, angle width, aperture of the transmitter and the receiver are the abovementioned factors. Further, briefly described the behaviour of the system model. In [30], discussed the internal parameters of the FSO communication and it is detailed explanation of wavelength effect, appropriate detectors, beam width and angle and type of modulation. Also, discussed the maximum possible coverage of the link and availability.

2.2 Visible Light Communication (VLC)

With the growth of the population, communication became the necessity of the day to day life. Also, university, home and office environments are broadly used in the present. Wired and wireless communication is used in the above-mentioned environments and wireless communication is the most favourable method due to practical comfortably. The existing RF bandwidth is not satisfied to present communication requirements such as mobile phone network, bluetooth and Wi-Fi. Therefore, scientists and researchers are move to OWC and VLC and IR are a subset of the OWC [1].
The several key problems identified in RF communication. The first key problem is capacity. With the expansion of the 5G and 6G communication, the RF frequency is limited. The second key problem is efficiency. The 7.1 billion mobile phone users are available worldwide. Due to consuming more energy, the efficiency is degraded. The third key problem is availability. There are several applications which unable to use RF such as power plants, aircraft and chemical applications. The fourth key problem is security. RF can infiltrate through objects and walls. Therefore, RF technology is a distrusted method for high-security applications. However, VLC can overcome the four key problems. The VLC is 10,000 times greater than the RF spectrum. Also, it uses very low energy and efficiency is high. Availability of the VLC is high due to all the indoor environments using LED lights. The light waves need LoS condition and they can't go through walls and objects. Then VLC has more security [31].
VLC is a novel technology in wireless communication that help to illuminate and at the same time the VLC technology data transfer using lightwave. VLC work on the visible light range and its belongs frequency range is from 430 THz to 790 THz and wavelength range is from 380 nm to 750 nm [32].

2.2.1 Advantages of VLC

In this section, we discussed the importance of lightwave communication and its advantages [33] - [34].

- Safety for human health
  The World Health Organization (WHO) mentioned that RF waves are affected by human health and can reason for cancer. Though, VLC technology used in LED and LED is harmless for human health.

- Use of existing infrastructure

At present in all places are used light bulbs for the illumination purpose. Therefore, existing infrastructure is used for illumination as well as communication.

- Wide bandwidth
  The RF spectrum has limited frequencies and it is up to 300GHz. Additional bandwidths are highly cost in the frequency spectrum. Also in RF high-frequency equipment are expensive. Therefore VLC is an advantage over the RF.

- Low cost
  The VLC used an unlicensed spectrum and no cost for the frequencies. VLC can use existing infrastructure and have a very low cost for implementation. The transmitter and receiver components are low priced.

- Use restricted area
  There are many places to communication is restricted such as hospital theatres, aircraft and some military applications. The RF signal interferes with equipment and VLC light communication can use those restricted areas.

- High data rate communication
  The VLC technology is communicating in the terahertz range of frequencies. Also, the data communication speeds of 100 Gbps and RF communication speeds of 1 Gbps.

- Green communication
  The VLC technology helps to reduce the pollution on earth. In light communication not use natural sources to produce energy to communicate.

2.2.2 VLC Applications

There are several applications are discussed in this section [1], [31], [33] [34], .

- Airline communication
  The Federal Communication Commission (FCC) is restrict to the use of the internet and mobile communication due to ground network inference and interference with avionics. However, there are several lights in the aircraft and VLC technology is easily used for indoor communication without any interfere.

- Healthcare
  There are a few limitations use Wi-Fi in the operation room in the hospitals such as radiation and it is interference with mobile phones & computers. However, VLC is the best option to overcome this issue.

- Underwater communication
  At present, Underwater Autonomous Vehicles (UWAV) are operated using cable connections with the ship. Also, submarines are communicated with ships using RF and submarines should come to the surface of the water to communicate. RF is not working underwater due to the absorption of the signal. However, lightwaves can go through the water medium and can communicate with UWAV and the ship.

- Vehical to Vehicle (V-to-V) communication
  VLC can use V-to-V communication with LoS. Using headlights and back-lights can communicate V-to-V as well as the vehicle to traffic signals. VLC helps to reduce traffic and increase the management of traffic.

- Hazardous environment
  In the power plants monitoring temperature, demand and intensity of the grid. Power plants use data systems to transmit all the details of the plant. When using the RF for the power plant communication purpose it made electromagnetic interference throughout the power plant. Therefore, VLC is a good option for us in a hazardous environment like a power plant.

- High-speed technology
  The speed of the Wi-Fi connection is up to 1 Gbps. However, VLC speed can be extended up to 100 Gbps.

- Device connectivity
  In VLC indoor communication is the most helpful application for interconnecting with smart devices such as laptops, smartphones and tablets. This connectivity is supply high data rates and security.

- Smart toys
  At the present, there are a lot of toys that use LED. Hence, VLC can implement to communicate with each toy.

- Analysis of supermarket
  The supermarkets have rich lighting facilities and use that lighting environ-

ment to implement the VLC system. Using VLC technology, each customer can be followed and detect the entire shopping progression.

2.2.3 Transmitter - LED in VLC

The LED was invented in the 1960s, with a single colour. With time it was changed into increased lifetime, small sizes, different colours, high response and high luminance. After many decades, LED technology has improved such as lu-

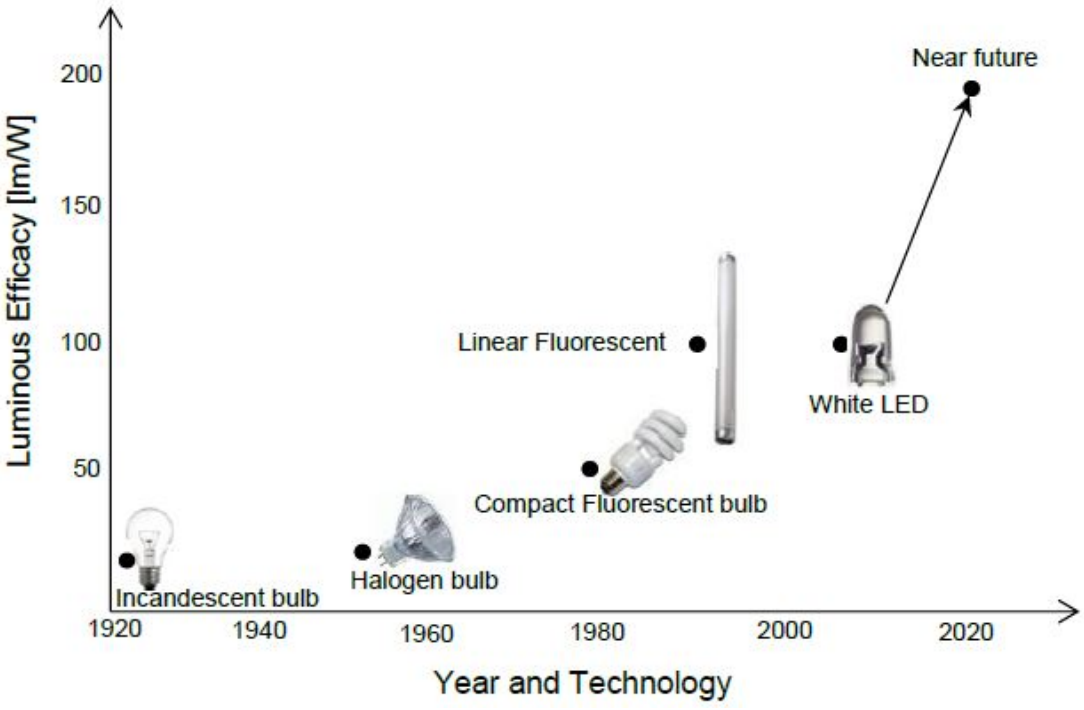

Figure 2.1: Luminous efficacy evolution of different light sources [3] .

minance increased by 20 times every 10 years, 1% price decreased by every 10 years. All upgrading positively affected the society and technology used for functions the everywhere. Figure 2.1 shows the evolution of the light sources over years.

LED has large benefits when compared to the bulb such as low cost, great efficiency, saving energy, low power consumption. When compared to the existing light like energy-saving lights and incandescent lights, the LED has 1/10 th power consumption and $\frac{1}{4}$ th save energy. Also, LED can reach 249 lm/W [35].

Figure 2.2 shows the working principle of the LED. The LED is a semiconductor and active electronic component. The difference between the diode and the LED is which LED can emit the light. A bias voltage is applied to the P-N junction and holes and electrons move towards. Connecting with electrons and holes the

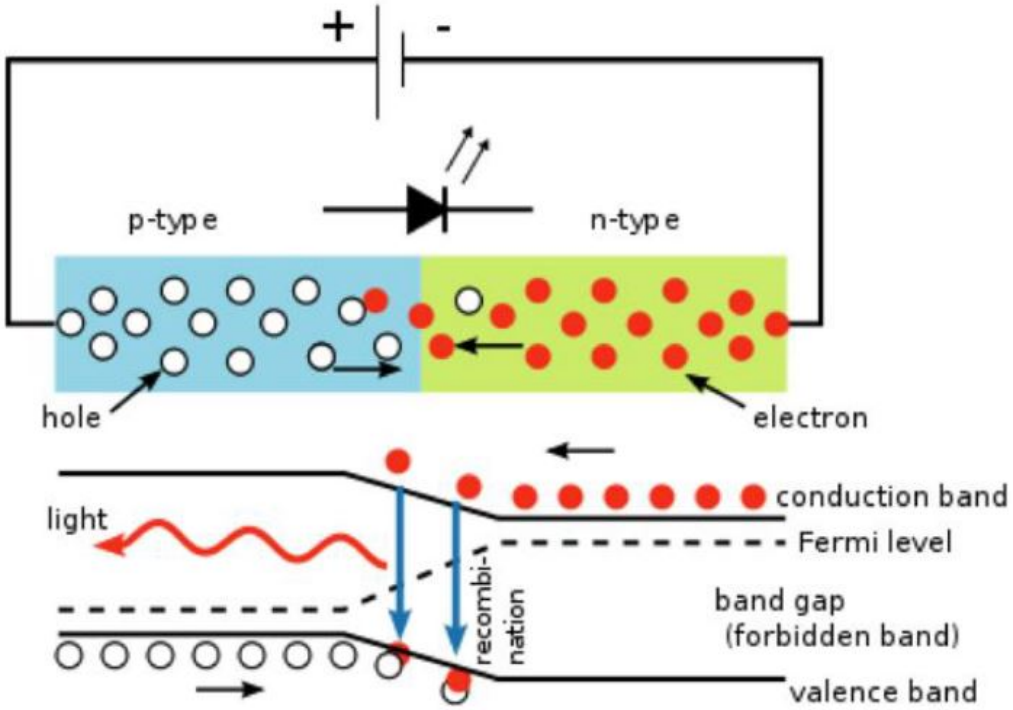

Figure 2.2: Working principle of LED [4].

depletion layer becomes thin and emits the lights. However, the electrons recombine with the holes and the electrons move the conduction band to the valence band. This process releases additional energy. Generally, Aluminium Gallium Arsenide is used as the material in LED. The most important factor of the LED is the material used to construct and LED colour is depends on the material. Table 2.1 represents the materials are used to construct the different colour LED and wavelength.

Material	Wavelength	Colour
Gallium Arsenide	850-940nm	Infra-Red
Gallium Arsenic Phosphide	630-660nm	Red
Gallium Arsenic Phosphide	605-620nm	Amber
Gallium Phosphide	585-595nm	Yellow
Indium Gallium Aluminum Phosphide	550-570nm	Green
Silicon Carboide	430-505nm	Blue
Gallium Nitride	450nm	White

Table 2.1: The materials to generate different colours of LED with wavelength

Initially, the LED material bond is strong and conducting the current is difficult. After adding the impurities the material imbalanced and form the holes and

electrons. The LED has a direct gap and no change in the momentum. Therefore, excess energy is released as light. The band gap energy is given by [5],

$$E_g = hf, \tag{2.1}$$

where h is plank constant and f is frequency.

$$f = \frac{c}{\lambda} \tag{2.2}$$

where c is the speed of lights and it is $3 * 10^8\ ms^{-1}$ and λ is wavelength.
The internal quantum efficiency of the LED is the ratio of the number of photons released to the number of electrons added.

$$\eta_{eff} = \frac{\eta_{re}}{\eta_{add}}, \tag{2.3}$$

where η_{eff} denotes the internal quantum efficiency, η_{re} denotes released photons and η_{add} denotes the added electrons.
The LED emission pattern depends on the surface material of the LED. The surface material depends on the refractive index of the material. Also, the emission pattern is modelled according to the Lambartian law. Using Snell law explain the refraction of the air and the LED material.

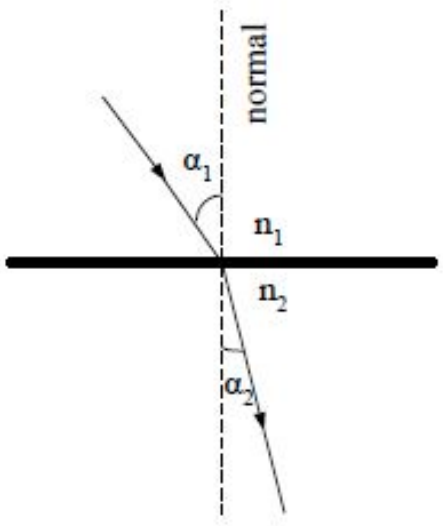

Figure 2.3: Refraction of the two different material.

Figure 2.3 represent the refraction scenario of the two different materials. Also,

mathematical model of the Snell's law represent using equation 2.4.

$$n_1 sin\alpha_1 = n_2 sin\alpha_2 \tag{2.4}$$

where n_1 and n_2 are two different materials and α_1 & α_2 are angles of the medium [5].

LED is a faster switching component as ON and OFF status and functioning speed is less than 1 μs. However, the LED seems continuously ON. Therefore, LED can use as an illumination component as well as data transmission using binary codes. For binary "1', LED is ON state and binary "0" is OFF state [31]. There are several types of LEDs such as Phosphor Converted (pc) $\breve{}$ LEDs, μ LEDs, Organic LEDs (OLEDs) and multichip LEDs. The pc$-$LEDs is blue light and it can convert pat of blue into green, red and yellow. However, phosphorous has a low response and has a limited band. pc$-$LEDs are low cost and low complexity. μ LEDs are used for parallel communication. It has high-speed switching compared with other LEDs. OLEDs are applied for a flexible devices like smartphones. A series of thin organic films are used to construct the OLEDs. To construct the multi-chip LEDs, use more chips to emit different colours. The colours can control individually by changing the intensity of each chip.

To obtain the general idea of the ideal LED, equation 2.5 introduce the Shockley equation and given by [4],

$$i_d = I_s(e\frac{v_d}{KT} - 1), \tag{2.5}$$

where i_d is the diode current, I_s is saturation current of the diode, K denotes the Boltzmann constant, V_d is the voltage across the P-N junction and T is the temperature in K. In equation 2.5 gives the I(V) characteristics of the forward bias and the reverse bias of the ideal diode.

In [36], this paper explained the long-distance communication in VLC technology. There are two data analog and digital. Using internal Field Programmable Gate Array (FPGA) communicate data through light waves. This system has reduced the complexity of the VLC technology and increase the distance between Tx and Rx. In [37], discussed the Multiple Input Multiple Output (MIMO) of the indoor VLC technology and considered relationship of FoV of transmitter and receiver, distance between two LEDs, area and process of switching.

In [38], this wok discussed the effect of the Lambertian's mode number and it depends on the FoV of the transmitter. The transmitter characteristics rely on the

Lambertian's mode number and FoV of the transmitter. Also, the receiver characteristics rely on the physical area of the PD and FoV of the PD. In [39], this work explained the comparison between Lambertian's intensity and non-Lambertian's intensity. Also discussed the advantages of both system model. In [40], explained NLoS in indoor communication and optimized the Lambertian's mode number. Also, considered four transmitter points and one receiver point with multipath dispersion. Using optimization, bandwidth and received power can improve.
In [41], this paper discussed the video transmit using VLC. The video can transmit about 10-15m using lightwaves. Using a microcontroller practically implement the transmitter and receiver. In [42], discussed the transmitter and receiver performance Further, The SNR depends on the transmitter performance and receiver arrangements. This paper expressed the details of arrangements and how it is affected by the SNR and BER.

2.2.4 Transmitter-Modulation Techniques used in VLC

The VLC technology used Intensity Modulation and Direct Detection (IM/DD). The changing the intensity of the LED and modulated the information signal. IM is non-negative. There are two carrier modulation schemes such as single-carrier and multi-carrier. The single carrier modulation techniques are On-Off Keying (OOK), Pulse Amplitude Modulation (PAM), Pulse Position Modulation (PPM) and multi-carrier modulation techniques are Orthogonal Frequency Differential Modulation (OFDM) [4].
OOK Modulation − According to the light communication standards, IEEE 802.15.7 and IEEE 802.11.bb are detailed in the OOK modulation scheme for VLC communication. The OOK modulation is the simplest modulation scheme with two states. It is simply called Binary Amplitude Shift Keying (BASK) modulation. The voltage presence use digital state '1' & the voltage absence use digital state '0' [33].

Variable Pulse Position Modulation (VPPM)˘There are two modulation types in VPPM such as Pulse Position Modulation (PPM) and Pulse Width Modulation (PWM). The PPM change the only position of the pulse and it has constant width and amplitude of the pulse. With the PPM modulation scheme, one pulse is used for one bit and the data rate is limited. Also, the PPM is easy to implement. PWM signal varied the width of the signal. PPM helps for communication and PWM helps for dimming conditions [31]- [33].

Colour Shift Keying (CSK)− This is based on the intensity of the RGB colours using chips. The data is transmitted according to the change of colour. Also, different colours can be created using the basic colours of RGB. The complexity is the main disadvantage of the system [41].

Orthogonal Frequency Division Multiplexing (OFDM)-The OFDM scheme is allocated subcarriers to send the information Tx to Rx. Also, avoiding the inter symbol interference is the advantage of the use of OFDM [33].

In [43], this paper the comparison between different modulation schemes such as Pulse Width Modulation (PWM), PPM, CSK, OOK and OFDM. PWM showed high BER at low SNR and it had the lowest data rate. PPM displayed high BER for the medium SNR and it presented a low data rate. CSK had low BER at medium SNR and it is presented a medium data rate. Further, OOK showed the lowest BER at high SNR and it is presented medium data rate.
In [44], this journal used basic OFDM index modulations and introduced two subcategories in OFDM modulations such as Sparse Activated Subcarriers OFDM Index Modulations (SAS-OFDM-IM) and Interpolated Sparse Activated Subcarriers OFDM Index Modulation (ISAS-OFDM-IM). With a comparison between conventional modulation schemes and proposed modulation schemes, BER is decreased in 5dB. Further, proposed modulation scheme can be improved spectral efficiency.
In [45], this work introduced a new modulation scheme called Generalized Spatial Pulse Position Modulation (GSPPM). The proposed modulation scheme is compared to the conventional modulation schemes such as PPM, Space-Shift-Keying (SSK) and Spatial Pulse Position Modulation (SPPM). This paper showed GSPPM outperforms PPM and SSK.
In [46], this paper explained the proposed method to avoid the inter sysmbol interference of the VLC system. Also, discussed the feed-forward pre-equalization with PAM modulation. It is used in VLC technology due to the bandwidth limitations of the LED. The purposed system forward pre-equalization with PAM modulation outperforms the Non-Return Zero (NRZ) modulation.
In [47], this paper implemented VLC technology in indoor communication system. Further, it is considered two modulation schemes such as OOK and PSK. The PSK modulation scheme can be achieved a longer distance compared with the OOK modulation scheme.
According to IEEE standards for the VLC (IEEE 802.11 and IEEE 802.15.7) and

IrDA standard suggested OOK and VPPM modulations for the physical layer I and physical layer II. Also, 4-CSK, 8-CSK and 16-CSK suggested for physical layer III [48].

2.2.5 Receiver-PD/Solar Cell in VLC

Solar cell or photodiode plays the main role of the receiver end in OWC and the receiver converts the optical energy into electrical energy. The optical energy is detected by a photodiode and the mechanism is photoelectric effects to produce the electrical current. Edmond Becquerel has discovered the photo-voltaic effect and it is generating voltage or electric current. The N-type and P-type semiconductors are used to manufacture solar cells. The produce PN junction creates an electric field electrons flow to the P-side and holes flow to the N-side. The light generates photons and captivate by solar cells. In this situation light particles of solar energy are photons. When the light comes and detects by solar cells, the free electrons move to the surface of the cell and generate holes due to moving the electrons. Continuously, happen this incident and more electrons and more holes create. In a solar cell, two plates ionize positively and negatively. Therefore, electricity is generates and use for ID and EH purposes. The solar cell must have a few requirements such as long lifetime, minimum temperature sensitivity, noiseless circuit implementation, small size, low cost and reliability [5]. In a solar cell, the quantum efficiency is a fraction of absorbed photons to the photocurrent. The photodetector responsivity is the fraction of the output current to the input power. The photodetector responsivity is given by,

$$R = \frac{I_p}{P_{in}}, \tag{2.6}$$

where I_p denotes the output current and P_{in} denotes input optical power.

On the receiver side, there are many features of solar cells and photodiodes such as fast response time, low noise, low price, wide bandwidth, small resolution angle, high efficiency and high responsivity.
When transmitting the signal from transmitter to receiver, different types of noises can be introduced in VLC technology. However, there is a difference between transmit signal and the received signal. When adding the noises to the transmit signal, the received signal quality is degraded. Therefore, we discuss the noises in wireless communication as well as VLC technology.
There are two types of noises such as input independent noise and input depen-

dent noise. The input independent noises are thermal noise and amplifier noise. The input independent noise is shot noise.

$$y = rhx + \sqrt{rhx}Z_1 + Z_0, \tag{2.7}$$

where r denotes optoelectronic conversion factor of PD. Z_1 denotes the input dependent noise and Z_0 denotes the input independent noise. The shot noise creates due to the thermal motion of electrons.This is an unavoidable electrons fluctuation. When applying the shot noise to the system electric current does not flow continuously. To avoid this issue can be used linear bandpass filter. The shot noise is given by,

$$I(t) = I_p + i_s(t), \tag{2.8}$$

where $I(t)$ denotes the instantaneous current of diode, $i_s(t)$ denotes the current fluctuation due to shot noise and I_p denotes the photo current. The variance of the shot noise is given by,

$$\sigma_s^2 =< i_s^2(t) > 2qI_pB, \tag{2.9}$$

where q is electronic charge and B is the effective receiver bandwidth.
Thermal noise creates naturally due to the temperature of the circuit. Also, it can be found in optoelectronic devices. Variance of the thermal noise is given by,

$$\sigma_T^2 =< i_T^2(t) > \frac{4kTB}{R_L}, \tag{2.10}$$

where K is the Boltzmann constant, T denotes the temperature of the receiver and R_L is the load resistor at the PD. [49]- [50].
Also, VLC technology faced the noises and it can be classified as Gaussian noise or shot noise. Noises follow a stochastic law and it has mathematical distribution. Gaussian noise follows the Gaussian distribution and shot noise follows a Poisson distribution. VLC technology faced the noises and it can be classified as Gaussian noise or shot noise. Noises follow a stochastic law and it has mathematical distribution. Gaussian noise follows the Gaussian distribution and shot noise follows a Poisson distribution. In general, two noises identified quantum noise and background radiation noise. The quantum noise can be identified as photon fluctuations. In brief, the photons fluctuation is the photons emitted from the light source and the emitting time is not constant. Further, the dark current noise is randomly generated noise due to electrons and holes in the detector. The

dark current depends on the energy gap and the material used to construct the detector. The background radiation noise is environmental noise such as ambient light and sunlight [51].
Further, we discuss the basic noise model AWGN use in information theory. It occurs in nature and randomly. Figure 2.4 shows how to add the AWGN to the

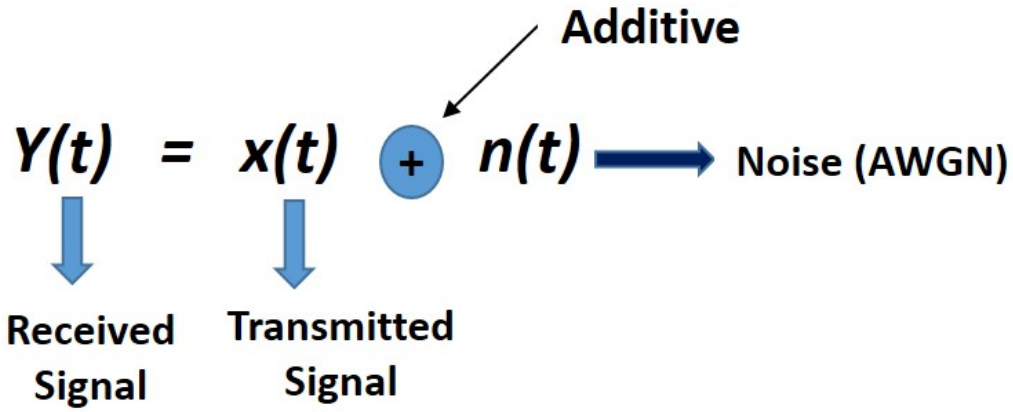

Figure 2.4: AWGN of the communication system model.

communication system model.

2.2.6 Channel Models in VLC

In [5], this paper discussed the configuration of the six VLC models such as direct LoS configuration, hybrid LoS configuration, non-direct LoS configuration, direct non-LoS configuration, hybrid non-LoS configuration and non-direct non-LoS configuration. The direct LoS configuration has rich received power and low interference with the artificial light source. The hybrid LoS configuration is not focused on to transmitter and receiver. Also, it has different directionalities. The non-direct LoS configuration needs a large FoV for the receiver as well as the transmitter. Direct non-LoS configuration, hybrid non-LoS configuration and non-direct non-LoS configuration are diffused systems and transmitted signals do not directly detect the receiver. Figure 2.5 shows the configuration of the channel models.

In [52], this paper discussed the LoS propagation model and the non-LoS propagation model of the multipath signal in VLC technology. The LoS propagation model outperforms the non-LoS propagation model. The non-LoS faced several difficulties such as more noise, reflection and scattering. However, LoS propaga-

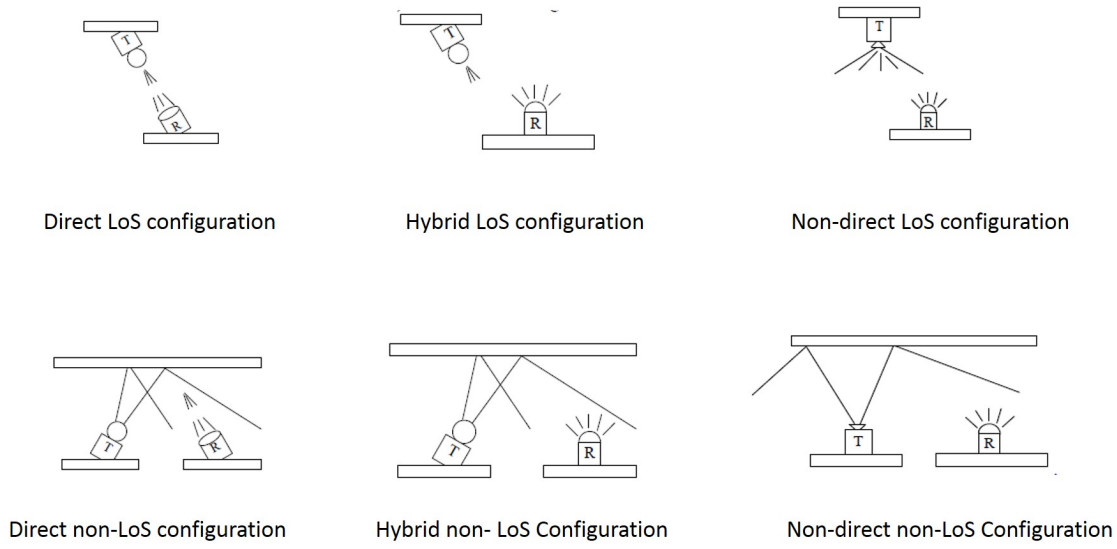

Figure 2.5: Transmitter and receiver configuration models [5].

tion model has good received power and less noise susceptibility than the non-LoS propagation model. In [53], this paper discussed k-th reflection of the light wave system model and considered the performance of the proposed design mathematically. Also, discussed the advantages and the disadvantage of the system model. Further, discussed the transmitter characteristics, size of the room, and LED mount design. In [54], this paper explained the positioning system of the LED in indoor communication and compares the cost, accuracy and environment of the different positioning systems.

2.2.7 Energy Harvest (EH)

Nowadays, EH is the most discussed topic and energy requirement is increasing day by day. Energy conversion or energy harvesting is ambient energy such as light, wind, RF and vibration converted to electrical energy. In a wireless communication environment, the EH process plays a major and useful role. Before that batteries and super capacitors help to supply power to the part of the wireless communication environment. However, applying the batteries to different environments is not easy such as sensor networks, toxic environments and the human body. Due to the high cost of the batteries, battery replacement is not a practical scenario. To improve the QoS of future wireless communication harvesting energy is more practical and more efficient. Further, EH helps to reduce e-waste and carbon waste [55]- [56].

2.2.8 Simultaneous Lightwave Information and Power Transfer (SLIPT)

The article [14], discussed the EH in VLC in indoor communication. The research work expanded to optimize the receiver side with a modern solar system with an increase in the conversion of the output level, optimize the battery. Also, discussed the VLC/RF hybrid communication system with EH harvesting relay. This work presented the SISO system and BER performance of the system with M-PAM technology. Also, used a multicarrier system with various modulation techniques. Finally, discussed the LED arrangement of the indoor environment and the reflection of the LEDs and discussed the future directions of the EH in VLC.

This work [57], discussed the receiver optimization and system simulation done using Matlab/Simulation. Here, measured the data rate, DC voltage of the receiver side, AC voltage of the receiver and optimized the amplifier circuit. However, it is not considered the channel influence and room light condition. This article [58], discussed the multi-users and evaluate the EH possibilities. It is considered the time division multiple access (TDMA) and optical intensity with time allocation for each user. Further, optimize the EH system and increase the QoS of the the system. Also, verified the optimal results of EH. In [59], considered indoor IoT applications with SLIPT technology. Further, it is discussed the SLIPT strategies and optimized the EH and maintaining with ID.

In [60], investigated outage performance of downlink and uplink scenarios in the RF/VLC hybrid system. Also, it is observed interference and non-interference conditions of the system. Using Monte-Carlo simulation simulated outage probability according to the analytical expressions. Also, considered rician fading channel for the system. In this article [61], discussed the VLC-RF proposed system and considered RF-EH. Also, investigated the outage probability of the VLC downlink. Also, observed outage probability of RF uplink. Finally, it is discussed rician fading channel with the randomness of the VLC downlink and EH through VLC. In this work [62], compared the existing EH systems such as ambient light sources, TV transmission and thermal energy. Finally, focused RF-EH and circuit design of harvester. In [20], investigated the harvested energy with information data rate, increased the number of transmitters (LED) and observed the behaviour of EH with information decoding data rate. Further, consider the effect of the FoV of the transmitter and the receiver on EH and ID.

This work [63], considered the channel capacity of the SLIPT system and observed the effect to the achievable information data rate. Also, discussed the transmitter

output current and voltage, amplifier output of the solar panel. Further, it is discussed the multi transmitters and multi receivers of the SLIPT system. Finally, it is explained the minimum EH requirement. In [64], introduced SLIPT receiver architecture and cooperative communication in the MIMO SLIPT system. Also, the physical layer protection is discussed and investigated. Further, improve methods to protect the physical layer. Finally, discussed the future directions of the SLIPT system.

2.2.9 Simultaneous Wireless Information and Power Transfer (SWIPT)

SWIPT is a trending topic in wireless communication and a new era begin with 5G communication. With the improvement of technology, the essential need is power efficient systems. Also, smaller in size in new equipment. The SWIPT is the transfer of information and power from the transmitter to the receiver. In [65], provided the details of the overview of the SWIPT system. Also, it explained the future directions of the SWIPT technology. In [66], explained communication protocols and smart antennas in the SWIPT technology. The basic receiver architecture designs are discussed in [67]. In [68], discussed the theoretical aspects as well as the practical aspects of the SWIPT system and physical layer effects. In [69], discussed the interference issues for the SWIPT technology and explained to manage the interference when using the technology.SWIPT research challenges and features of the energy sources have discussed in [70]. In [71], discussed the limitations of the SWIPT EH and reviewed finite, zero, infinite batteries. Further, introduced a new optimization method of the batteries. In [72], explained the theoretical background of the RF-EH and discussed the WSN with power transfer. In [73], discussed the wireless body sensor network and limitations. Further, presented a detailed review of the EH support body sensor network. Also, discussed the sources of harvested sources.

The article [17], provided the details of the SWIPT concept, interference affected to the SWIPT technology. Further, discussed Multiple Input Single Output (MISO), Multiple Input Multiple Output (MIMO), WSN, multi-carrier and cooperative communication. Also, explained the theoretical and practical frameworks with channel coding, hardware impairments of the SWIPT system. Finally, they discussed the future directions with modern technologies such as IoT and satellite communication of the SWIPT technology.

2.2.10 Limitations of the VLC

Several limitations can be identified in VLC technology. VLC has multipath dispersion in transmitter and receiver detect the information in various ways. Also, multipath dispersion is directly affected by the SNR [3]. There are several reflective surfaces in indoor communication such as doors, walls, ceilings and windows. Further, the receiver is sensitive to ambient light sources and background noise with difficult to detect correct information that sends by the transmitter. Finally, the PD sensitivity is proportional relates to the area of PD. However, PD has limitations to extend the area due to receiver size for relevant applications [63].

2.2.11 Chapter Summary

In this chapter, we extend our knowledge to the OWC and FSO to get the basic idea of lightwave communication. Moreover, we study the transmitter, receiver, channel model, modulation techniques, advantages, applications, a basic principle of LED, the basic principle of PD, the evolution of light sources of VLC. Also, study the VLC existing research and ongoing research. Further, study the concept of EH and current methods of the EH. Also, study the RF-EH(SWIPT) and VLC EH (SLIPT).

Chapter 3

SYSTEM MODEL

In this chapter, we present the overview system model of the SLIPT architectures. Initially, we discuss the VLC system model with LoS, mathematical model of the transmitter, free space channel model and receiver. Also, explain the Lambartian's mode number and FoV of the LED and the PD. Moreover, we explain the transmitter change from the electrical domain to the optical domain and the receiver change from the optical domain to the electrical domain. Further, we discuss the SLIPT receiver architectures such as the PS SLIPT receiver model and TS SLIPT receiver model. Also, we explain the mathematical model of the AC component in the SLIPT architecture to ID and the mathematical model of the DC component in the SLIPT architecture to EH. Finally, we explain in this chapter the SWIPT system model and SLIPT system model for indoor communication. Also, we discuss outage probability in the mathematical model for both systems.

3.1 VLC System Model

In this section, we discuss the basic system model of VLC. Further, the Chapter 1 - Section 1.2 explain the basic introduction of the VLC system. Figure 3.1 shows the basic system model of the VLC and consider LoS between the Transmitter (Tx) and the Receiver (Rx). This system model uses a wireless communication channel and it is free space. Also, it performs as a medium between Tx and Rx and it has high bandwidth and does not require a licence for spectrum. The α denotes the FoV of the LED, θ denotes the PD and d is the distance between Tx and Rx.

Figure 3.2 shown the overall system model of the SLIPT system. It shows the variation of one domain to another domain. There are three parts of the system, namely transmitter, channel and receiver. The transmitter includes an information signal, modulator, converter circuit of electrical signal into an optical signal and LED. The information signal is transmitted as binary data ($m(t)$) and

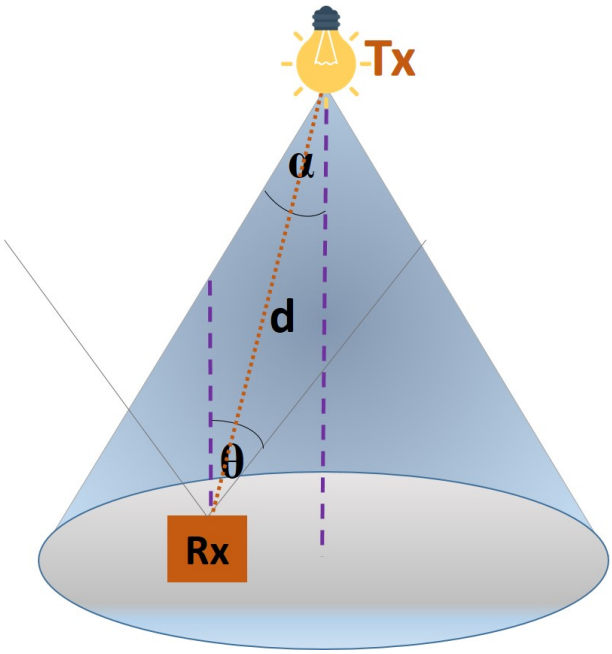

Figure 3.1: Basic system model of the VLC and LoS between Transmitter (Tx) and the Receiver (Rx).

used the modulation techniques to modulate the signal ($m'(t)$) to send the E to L driver circuit. On-Off Keying (OOK) modulation technique generally used for the VLC communication. Using the drive circuit, convert the electrical signal into an optical signal. Also, LED helps to send the optical signal to the receiver. Moreover, the h is the channel gain coefficient between the transmitter and the receiver with AWGN. The AWGN ($n(t)$) is a basic noise model is used for the information theory to follow the effect of the many random process that occur in nature in wireless communication.

The receiver includes PD or solar cell, the converter circuit, demodulation and the output data. The PD or solar cell detects the optical signal and send it to the L to E driver circuit. Using the drive circuit, convert an optical signal into an electrical signal and used demodulate to output data.

The basic mathematical equation for the overall system given as follows,

$$y(t) = hm(t) + n(t), \tag{3.1}$$

where y(t) denotes the output of the overall system, h defines the channel gain, m(t) denotes overall inputs and n(t) denotes the overall noises in the system. In general, two basic noises affect by the optical systems as input independent noises and input dependent noises. Shot noise is the input dependent noise. Also, it causes by the thermal motion of the electrons and occurs in any conductor that

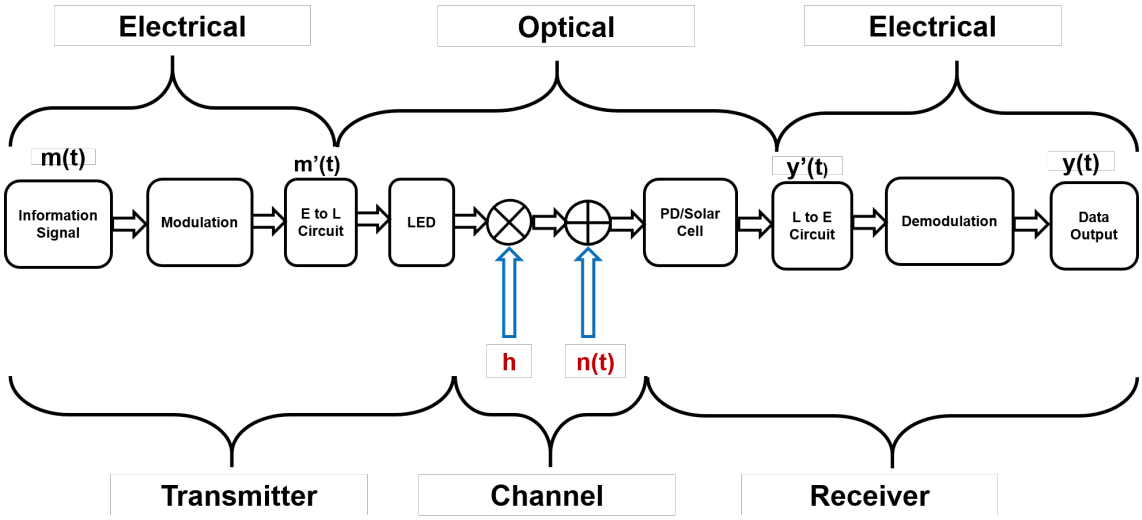

Figure 3.2: Block diagram of the overall system model of the VLC.

has a resistance. Further, shot noise results from the fact that the current is not a continuous flow. The thermal noises and the amplifier noises are the input independent noises in optical communication. Also, thermal noise is caused by the thermal motion of the electrons inside the electrical circuits. In communication, thermal noise has a major influence on the quality of the receiver.

3.1.1 Mathematical Model for the VLC Transmitter

Transmitted optical power is given by [20],

$$P_t(t) = P_{LED}[B + m'(t)], \tag{3.2}$$

where P_{LED} is the LED power per unit (in W/A). B denotes the adding DC bias signal and m'(t) is the modulated electrical signal. B is the DC component and m'(t) is the AC component of the signal.

3.1.2 Mathematical Model for the Free Space Channel

In this Section, we discuss the free space channel between transmitter and receiver. The channel gain also in consideration to system design and can be expressed as [74],

$$h = \frac{A_r(m+1)(cos^m(\alpha)T(\theta)g(\theta)(cos(\theta)}{2(\pi)(d^2)}, \;\; 0 \leq \alpha \leq \pi, \;\; 0 \leq \theta \leq \pi, \tag{3.3}$$

where d is the distance between the transmitter and the receiver, $T(\theta)$ defines the optical filter gain and A_r denotes as the physical area of the detector at the receiver end. The α denotes the FoV ($0 < \alpha < \pi$) and it is represents as the angle of irradiance of LED. The θ denotes the FoV ($0 < \theta < \pi$) and it is represents as the angle of incidence of LED.

$$m = \frac{-ln(2)}{ln(cos(\alpha))}, \qquad 0 < \alpha < \pi, \tag{3.4}$$

where, m denotes the Lambertian's mode number and it gives the direction of the source.

Gain of the optical concentrator is given by [74],

$$g(\theta) = \frac{n^2}{sin^2(\theta)}, \qquad 0 < \theta < \pi, \tag{3.5}$$

In equation (3.5), n denoted as the refractive index and $g(\theta)$ assign the optical concentrator gain.

3.1.3 Mathematical Model for the Receiver

In this section, we discuss the receiver of VLC system model.

$$P_r(t) = hP_t(t), \tag{3.6}$$

where $P_r(t)$ is the receive power and $P_t(t)$ is the transmit power.

The received signal expressed as,

$$y(t) = \sqrt{P}hm(t) + [n(t)\sqrt{\sigma}_{tot}], \tag{3.7}$$

where, σ_{tot} is the noise power of the transmitter and the receiver.
In the Chapter 4 - Section 4.1.1 include the numerical results of the FoV of transmitter and receiver to achieve maximum received power in VLC communication system. Also, in Chapter 4 - Table 4.1 mentions all numerical values for each FoV of transmitter and the receiver.

3.2 SLIPT Receiver Architectures

In this section, we discuss the SLIPT receiver architecture such as PS-SLIPT TS-SLIPT. Moreover, the Chapter 1 - Section 1.4 explained the introduction of the

SLIPT receiver architecture. Also, Section 1.4.1 and 1.4.2 introduced PS-SLIPT and TS-SLIPT respectively.

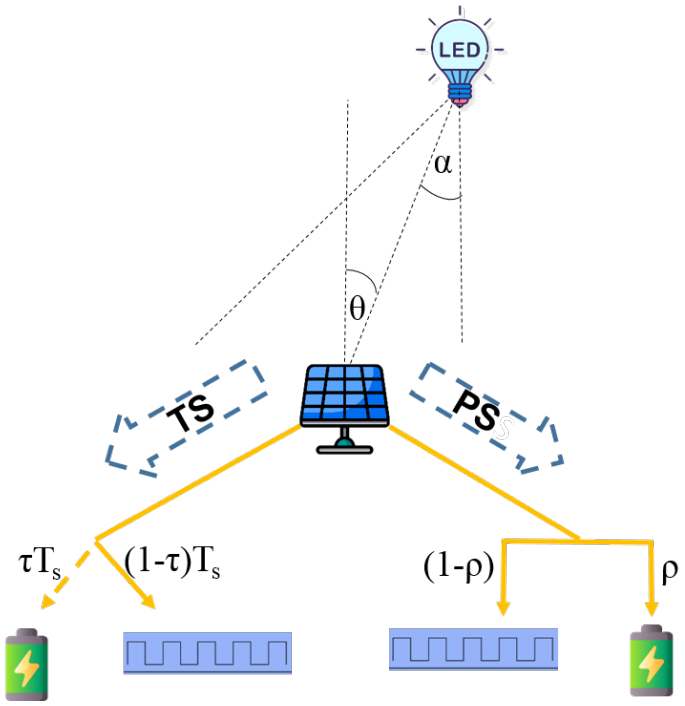

Figure 3.3: Overall system model of SLIPT system with PS receiver architecture and TS receiver architecture.

The SLIPT system builds on VLC technology and a diagram shown in Figure 3.3. The diagram shows the downlink SLIPT system with the transmitter, channel and receiver. On the receiving side, there are two functions as EH and ID. Further, the received signal divided into two portions: AC component and the DC component. The modulated signal gives an AC component and its support to transmit the information. Also, the DC component helps with energy harvesting.

In Figure 3.4 shows the transmission block diagram of the PS and TS architectures. Moreover, ρ is the power splitting coefficient and τ is the time splitting coefficient and P_r is total received power and T_s is the total time taken to transmit data.

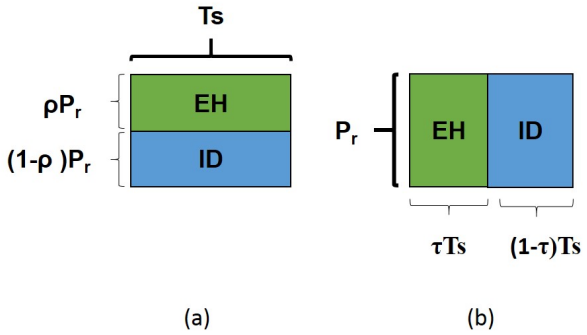

Figure 3.4: (a) PS SLIPT architecture shows the concept of dividing power for EH and ID. (b) TS SLIPT architecture shows the concept of dividing time for EH and ID.

3.2.1 Received Electrical Signal

Received electrical signal is given by [59],

$$i_r(t) = \eta h P_t(t) + n(t), \tag{3.8}$$

where η denotes the photo detector responsivity in (A/W). Photo detector responsivity is the ration of the generated photo current and incident or absorbed optical power. It is neglecting noise influence.

$$i_r(t) = I_{DC}(t) + i(t) + n(t), \tag{3.9}$$

where I_{DC} denotes the DC component of the received signal and i_t is the AC component of the received signal. Also, $n(t)$ denotes the AWGN.

3.2.2 AC Component of the Received Signal $i(t)$ - Information Decoding

The received signal for the ID is given by [59],

$$i(t) = \eta h(1-\rho) P_{LED} m'(t), \tag{3.10}$$

where $i(t)$ is the AC component of the signal.

$$\gamma_{PS} = \frac{(\eta h(1-\rho) P_{LED} A)^2}{\sigma^2}, \tag{3.11}$$

where the amplitude of the transmitted signal denotes A and ρ is the PS coefficient. σ^2 denotes the noise power (thermal noise and shot noise).

Also, the SNR for TS SLIPT system can be expressed as follows ,

$$\gamma_{TS} = \frac{(\eta h P_{LED} A)^2}{\sigma^2}, \tag{3.12}$$

The information rate of channel using PS SLIPT system is expressed as,

$$R_{PS} = W T_s log(1 + \gamma_{PS}), \tag{3.13}$$

Also, information rate of channel using TS SLIPT system is expressed as,

$$R_{TS} = (1 - \tau) T_s W log(1 + \gamma_{TS}), \tag{3.14}$$

where W denotes the system bandwidth.

3.2.3 DC Component of the Received Signal I_{DC} - Energy Harvesting

The amount of harvested energy is given by,

$$E = f \rho I_{DC} V_{oc}, \tag{3.15}$$

where f is the fill factor (FF). **FF** is defined overall behaviour of a solar cell and it is measure of quality of a cell.

$$I_{DC} = \eta h P_{LED} B, \tag{3.16}$$

The open circuit of voltage is given by,

$$V_{oc} = V_t ln(1 + \frac{I_{DC}}{I_0}), \tag{3.17}$$

where V_{oc} denotes the open circuit voltage of solar cell and V_t denotes the thermal voltage. Thermal voltage is the voltage which produced within P-N junction due to the action of temperature. Also, I_0 is the dark saturation current of the photo diode and it is the reverse leakage current of the diode.

Therefore energy harvesting for PS system equation is expressed as,

$$E_{PS} = f T_s (\eta h \rho P_{LED} B) V_t ln(1 + \frac{\eta h \rho P_{LED} B}{I_0}), \tag{3.18}$$

where E_{PS} denotes the harvested energy from PS-SLIPT architecture while decode the information.

The energy harvesting for TS is expressed as,,

$$E_{TS} = f\tau T_s(\eta h P_{LED} B)V_t ln(1 + \frac{\eta h P_{LED} B}{I_0}), \tag{3.19}$$

where E_{TS} denotes the harvested energy for TS receiver architecture.
In Chapter 4 - Section 4.1.2 included the simulation results of the BER for different modulation schemes in PS-SLIPT architecture. Further, Section 4.1.3 included the behaviour of the information decoding data rate vs splitting coefficient in PS and TS SLIPT architectures. Also, Section 5.1.4 included the behaviour of the energy harvesting vs splitting coefficient in PS and TS SLIPT architectures. Moreover, Section 4.1.5 included the behaviour of the energy harvesting vs information decoding in PS and TS SLIPT architectures for different bias values and Section 4.1.6 included the sub-optimal splitting coefficient with BER in PS and TS SLIPT architectures under AWGN.

3.3 A SLIPT-Assisted Visible Light Communication Scheme

In this section, we discuss the SWIPT system and SLIPT system. Further, we explain the SWIPT system model is SM-I, and the SLIPT system model is SM-II. Moreover, we describe the mathematical model of both systems for ID and EH. In the proposed system models, a source and a destination communicates with a direct link using SWIPT and SLIPT schemes. An overview both of the system models referred by Figure 3.5.

3.3.1 SWIPT System Model: SM-I

In this section, we discuss the SWIPT system model. Further, the Chapter 1 - Section 1.5 explained the basic introduction of the SWIPT system.
According to PS process in SWIPT protocol, the received signal divides into two fractions where the first fraction assigned of received signal to use for EH and the remaining is used for information transmission. The power splitting factor denoted by the symbol ρ. Thus, the received signal fraction in ρ is used for energy harvesting and remaining $(1-\rho)$ is used for information processing at the destination. The power splitting factor ρ directly affects the amount of energy harvested and total achievable throughput of the system. According to the system model, the source communicates with the destination with the signal power of P_t and received signal at the destination through direct link during the time period $t = T$ can be written as,

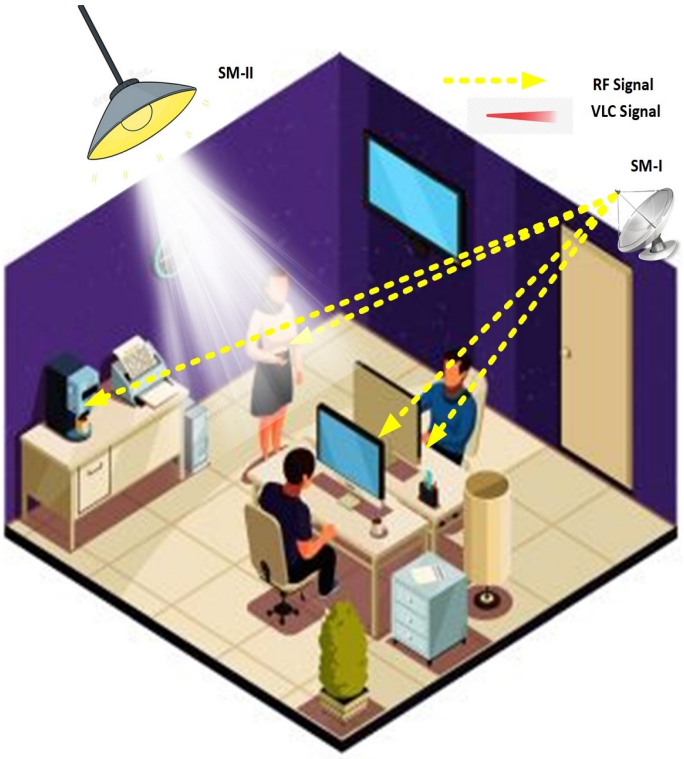

Figure 3.5: SWIPT and SLIPT System Model Scenario

$$y(t) = \sqrt{\frac{P_t}{d^k}} hm(t) + n(t), \tag{3.20}$$

where m represents the modulated symbol generated by the Binary Phase Shift Keying (BPSK) modulation technique, i.e $E\{|m(t)|^2\} = 1$, the channel fading coefficient is denoted by h along with the distance d between source to destination. The path loss exponent k depending on the channel conditions.
Thus, the received SNR at the destination given by,

$$\gamma_d = \frac{P_t |h|^2}{d^k \sigma^2}, \tag{3.21}$$

where σ^2 represents the variance of the AWGN at the direct communication link destination.

3.3.1.1 RF-Energy Harvesting in SWIPT Protocol

According to the system model, a power splitter equipped at the receiver end with a power splitting ratio of ρ:(1-ρ). The fraction of the received signal $\sqrt{\rho}y$ is used to EH while the remaining fraction of the received signal $\sqrt{(1-\rho)}y$ is used for information processing. Thus, the fraction of the received signal $\sqrt{\rho P_t/d^k} hm(t) + \sqrt{\rho} n$

is used to harvest energy while the fraction $\sqrt{(1-\rho)P_t/d^k}hm(t)+\sqrt{(1-\rho)}n(t)$ is used for information processing. An assumption has been taken that the energy harvested from the AWGN noise is negligible. Thus, the amount of harvested energy at the receiver end in the allocated time is be given by [75],

$$Er = \frac{\eta_e \rho P_s |h|^2 T}{d^k}, \tag{3.22}$$

where η_e represents the energy harvesting efficiency. The remaining fraction of the split signal is used for information processing and is expressed as,

$$y(t) = \sqrt{\frac{(1-\rho)P_t}{d^k}}hm(t) + n(t), \tag{3.23}$$

Thus, the SNR of the splitted signal $y(t)$ is given by,

$$\gamma_i = \frac{(1-\rho)P_t|h|^2}{d^k\sigma^2}. \tag{3.24}$$

3.3.1.2 Outage Probability Analysis for SM-I

The direct link outage probability of the indoor wireless system using SWIPT scheme can be expressed as,

$$p_{out}^{RF}(R) = Pr(log_2(1+\gamma_i) < R_{min}), \tag{3.25}$$

where R_{min} is the minimum achievable data rate in $b/s/Hz$ and γ_i is the instantaneous SNR of the SWIPT based indoor wireless system. By (3.23), some mathematical manipulations, the outage probability of the SWIPT system is simplified as,

$$p_{out}^{RF}(R) = Pr(\mid h \mid^2 < \underbrace{\frac{(2^{R_{min}}-1)d^k}{SNR(1-\rho)}}_{C}), \tag{3.26}$$

In this aspect the channel gain in this work has been taken as $x = |h|^2$ and follows the exponential distribution. The probability density function (PDF) further detailed and written as,

$$p_X(x) = \frac{1}{\sigma_x^2}\exp -\frac{x}{\sigma_x^2}, \tag{3.27}$$

where σ_x^2 denotes the variance of the channel coefficient. Additionally, the outage probability in (15) calculated in PDF as in (17),

$$p_{out}^{RF}(R) = \int_0^C \frac{1}{\sigma_x^2} \exp - \frac{x}{\sigma_x^2} dx, \tag{3.28}$$

The final expression of outage probability for SM-I in SWIPT protocol can be determined as,

$$p_{out}^{RF}(R) = 1 - e^{-} \frac{(2^{R_{min}} - 1)d^k}{SNR(1-\rho)}. \tag{3.29}$$

3.3.2 SLIPT System Model: SM-II

In this section we investigate a point−point communication link using SLIPT system. The transmitter convert the electrical power into optical power and receiver convert the optical power into electrical power [76]. As shown in Figure 3.4 the SLIPT system has two basic segment such as EH and ID. In SM-II, a LED used as the transmitter and in the receiver side a photodiode used for ID along with solar panel that is used for EH.

3.3.2.1 Outage Probability Analysis for SM-II

In SM-II, at the receiver end, the total received electric current can be expressed as [59],

$$i_{Rx}(t) = \eta(h(1-\rho)P_t(t)) + n(t), \tag{3.30}$$

where, $n(t)$ is the combined background shot noise and the receiver thermal noise modeled as an AWGN. The transmitted signal power $P_t(t)$ expressed mathematically as,

$$P_t(t) = \epsilon(\rho_{DC} + m(t)), \tag{3.31}$$

where ϵ denoted dimming factor, the BPSK modulated transmit electrical signal represented by $m(t)$ and ρ_{DC} described as the DC bias with peak amplitude of A which is added to the $m(t)$ for conversion into a non-negative digits. The received signal contained DC and AC components which can be further explained as,

$$i_{Rm}(t) = I_{DC}(t) + i_{AC}(t) + n(t) \tag{3.32}$$

In this work, the $I_{DC}(t)$ taken as negotiable, which will be used for EH. Thus, from the information perspective, only AC component is considered for outage

analysis and it can be written as,

$$i_{AC}(t) = i_t(t) + i_r(t), \tag{3.33}$$

where $i_t(t) = \eta h(1-\rho)P_t(t)$ represents the desired signal term and $i_r(t) = \eta P_r$ denotes the interference term. Accordingly, with the assumption of no interference, thus (3.32) can be further simplified as,

$$i_{AC}(t) = \eta h(1-\rho)P_r(t), \tag{3.34}$$

By substituting (3.33) in (3.31), the received electric current can be written as,

$$i_{Rx}(t) = \eta h(1-\rho)P_r(t) + n(t), \tag{3.35}$$

Finally, using (3.34), the instantaneous electrical SNR of the SM-II, the information receiver can be determined as,

$$\gamma_s = \frac{(\eta \epsilon h(1-\rho)A)^2}{\sigma_{tot}^2}, \tag{3.36}$$

where $P_t(t) = A^2$ defined the transmit optical power and the total noise variance for SM-II denoted by σ_{tot}^2

$$\sigma_{tot}^2 = (1-\rho)\sigma_{sh}^2 W + \sigma_{th}^2 W \tag{3.37}$$

The shot noise variance denoted by σ_{sh}^2, the variance of the thermal noise also denoted by σ_{th}^2 and W defined as the system bandwidth. By (3.24) and (3.25), the outage probability of the proposed indoor wireless system using SM-II, the information receiver considering LOS channel is computed as,

$$p_{out}^{VLC}(R) = 1 - e^{-}\frac{(2^{R_{min}} - 1)}{SNR(1-\rho)^2\epsilon^2\eta^2}. \tag{3.38}$$

In Chapter 4 - Section 4.2.1 included the simulation results of BER analysis of the SWIPT and SLIPT. Also, Section 4.2.2 included the Outage probability analysis of the SWIPT and SLIPT. Further, Section 4.2.3 included the amount of harvested energy in SWIPT and SLIPT.

3.4 Chapter Summary

In this chapter, we consider the basic three system models such as the VLC system model, SLIPT system model and SWIPT system model. The SLIPT model divides into basic two system models namely PS SLIPT receiver architecture and TS SLIPT receiver architecture. Further, this chapter explain the mathematical model for each system model such as ID data rate, EH and outage probability.

Chapter 4

RESULTS AND DISCUSSION

In this chapter, we present the simulation and numerical results of the propose system models of the SLIPT architectures. Further, analyze the FoV of the transmitter and receiver to achieve maximum received power in the VLC communication system and present the simulation results of BER for different modulation schemes such as OOK, QPSK and 8-PSK in PS SLIPT architecture. Also, we observe the behaviour of the information decoding data rate vs splitting coefficient in PS and TS SLIPT architectures and observe the behaviour of the energy harvesting vs splitting coefficient in PS and TS SLIPT architectures. Moreover, we observe the behaviour of the energy harvesting vs information decoding in PS and TS SLIPT architectures for different bias values, sub-optimal splitting coefficient with BER in PS and TS SLIPT architectures under AWGN, calculate the amount of harvested energy for optimal splitting coefficient and assume threshold SNR and analyze the PS and TS SLIPT architecture in energy harvesting and information decoding.
In addition, we explain the A SLIPT-assisted visible light communication scheme. It compares both SWIPT & SLIPT system models. Further, BER analysis of the SWIPT and SLIPT and outage probability analysis of the SWIPT and SLIPT system models. Moreover, we discuss the amount of harvested energy in SWIPT and SLIPT system models.

4.1 Performance Analysis of the SLIPT Architectures

In this section, we present the numerical and simulation results of the two receiver architectures such as PS SLIPT and TS SLIPT receiver architectures. We use the MATLAB for the simulations.

4.1.1 Optimal FoV Angle of TX and Rx

In this section, we obtain the numerical results of FoV of TX and Rx to achieve maximum receive the power of the VLC system model. The theoretical and math-

ematical background explain in section 3.1 and results explain under this section.

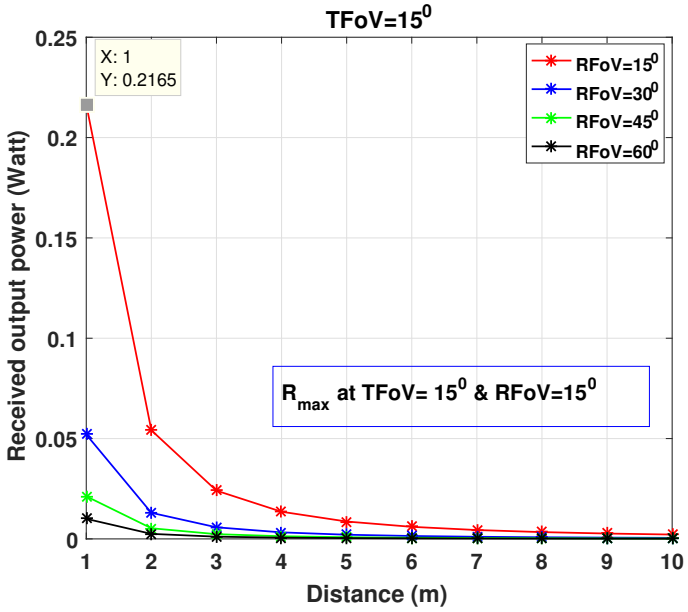

Figure 4.1: Transmitter FoV is 15^0 and Receiver FoV are 15^0, 30^0, 45^0, and 60^0.

Figure 4.1 shows the transmitter FoV is 15^0 and receiver FoV are 15^0, 30^0, 45^0, and 60^0. The maximum received power is given at TFoV at 15^0 and RFoV at 15^0 and the received power is 0.2165. Figure 4.2 shows the transmitter FoV is 30^0 and receiver FoV are 15^0, 30^0, 45^0, and 60^0. The maximum received power is given at TFoV at 30^0 and RFoV at 15^0 and the received power is 0.2421. Figure 4.3 shows the transmitter FoV is 45^0 and receiver FoV are 15^0, 30^0, 45^0, and 60^0. The maximum received power is given at TFoV at 45^0 and RFoV at 15^0 and the received power is 0.2601. Figure 4.4 shows the transmitter FoV is 60^0 and receiver FoV are 15^0, 30^0, 45^0, and 60^0. The maximum received power is given at TFoV at 60^0 and RFoV at 15^0 and the received power is 0.2065.

Table 4.1 shows the value of maximum received power with different values of TFoV and RFoV. According to the values in the table, we can observe the maximum received power is given at TFoV is 45^0 and RFoV is 15^0.

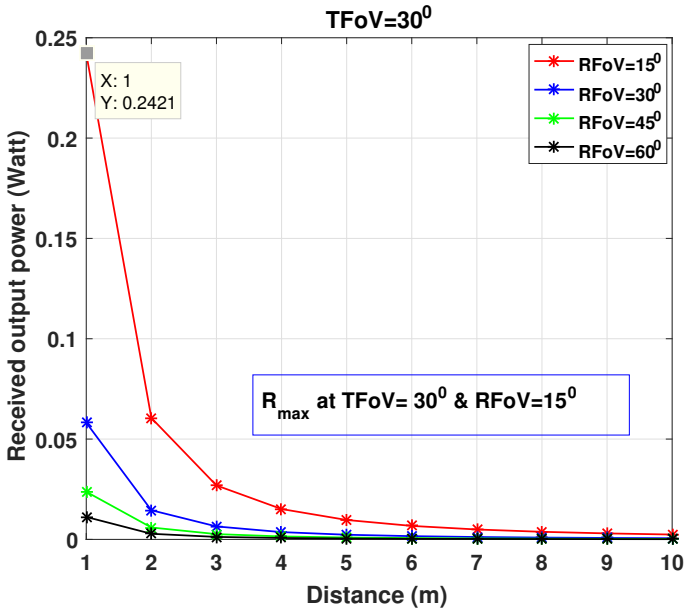

Figure 4.2: Transmitter FoV is 30^0 and Receiver FoV are 15^0, 30^0, 45^0, and 60^0.

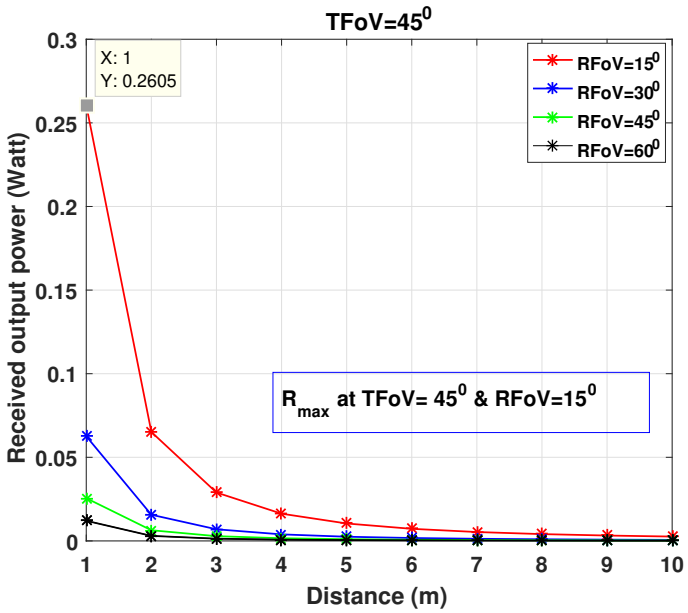

Figure 4.3: Transmitter FoV is 45^0 and Receiver FoV are 15^0, 30^0, 45^0, and 60^0.

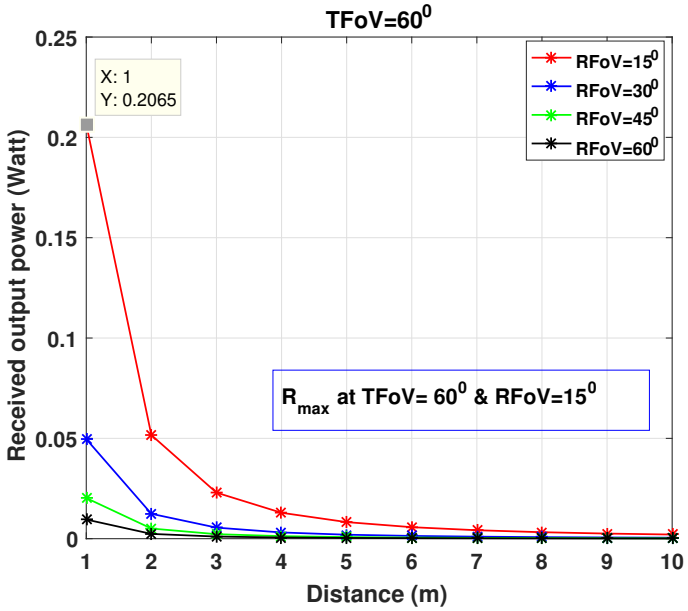

Figure 4.4: Transmitter FoV is 60^0 and Receiver FoV are 15^0, 30^0, 45^0, and 60^0.

Table 4.1: Maximum received power with transmitter and receiver FoV for 1m.

Transmitter FoV	Receiver FoV	Received Power (W)
15^0	15^0	0.2165
15^0	30^0	0.0520
15^0	45^0	0.0212
15^0	60^0	0.0101
30^0	15^0	0.2421
30^0	30^0	0.0582
30^0	45^0	0.0237
30^0	60^0	0.0112
45^0	15^0	0.2601
45^0	30^0	0.0626
45^0	45^0	0.0256
45^0	60^0	0.0120
60^0	15^0	0.2065
60^0	30^0	0.0496
60^0	45^0	0.0203
60^0	60^0	0.0095

4.1.2 BER Analysis in PS SLIPT Architecture Using Different Modulation Schemes.

There are a few reasons to over from analog modulation to digital modulation in wireless communication such as spectral efficiency, power efficiency, the robustness of channel impairment and the low-cost implementation. Digital modulation is transferring a digital bit stream over an analog channel at a high frequency. Moreover, digital communication schemes contribute to the evolution of wireless optical communication by increasing capacity, speed and quality.

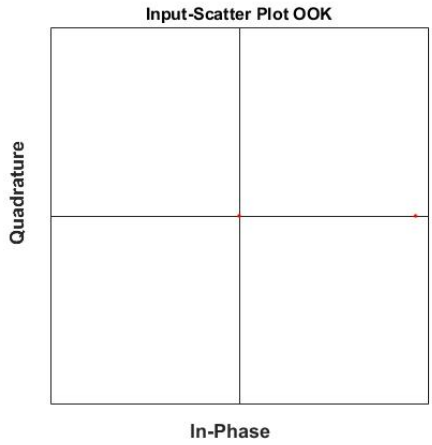

Figure 4.5: Input constellation diagram of OOK.

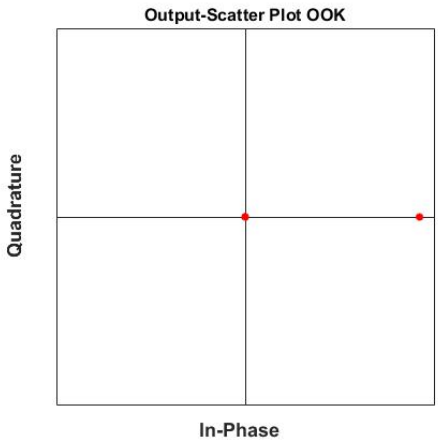

Figure 4.6: Output constellation diagram of OOK.

Figure 4.5 and Figure 4.6 show the input and output constellation diagram of the OOK modulation, Figure 4.7 and Figure 4.8 show the input and output constellation diagram of the QPSK modulation, Figure 4.9 and Figure 4.10 show

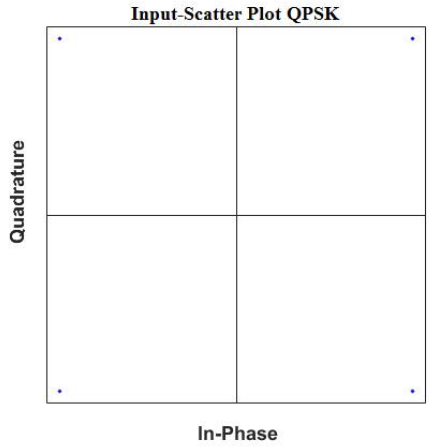

Figure 4.7: Input constellation diagram of QPSK.

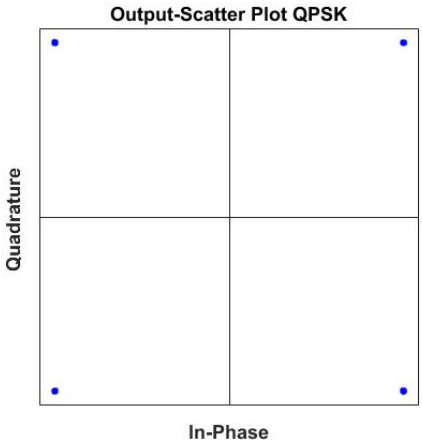

Figure 4.8: Output constellation diagram of QPSK.

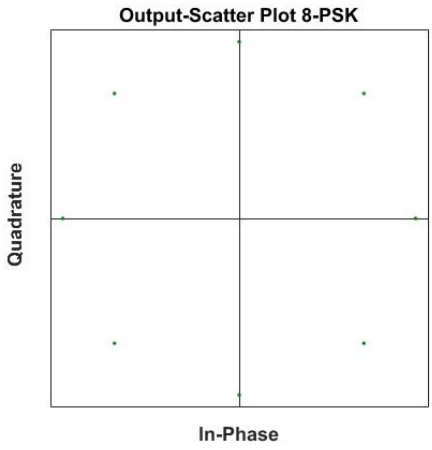

Figure 4.9: Input constellation diagram of 8-PSK.

the input and output constellation diagram of the 8-PSK and represent the affect of noises to the received signals at SNR is 30 dB at $\rho = 0.7$. The OOK is the

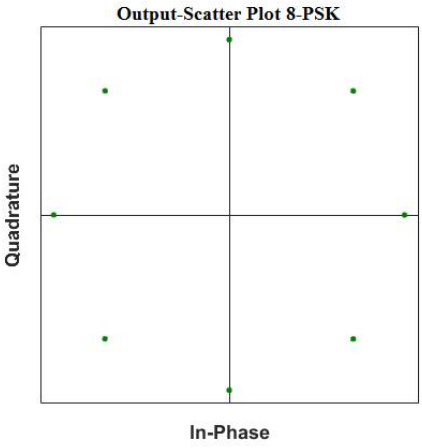

Figure 4.10: Output constellation diagram of 8-PSK.

amplitude modulation scheme commonly used in optical communication applications and it is a lower order modulation scheme. Further, we use two higher-order modulation schemes such as QPSK and 8-PSK. Both higher-order modulations are phase modulation. The M-PSK modulations use for this system to enhance the bandwidth efficiency and advantage is by using smaller phase shift, more bits can be transmitted per symbol. This system use AWGN noise and compared the input and output constellation of each modulation scheme.

The constellation diagrams represent symbols in digital modulation schemes. Using visual inspection of constellation diagrams can help diagnose various types of signal impairments. The constellation diagrams show the difference between input and output points. In this system, errors cause by transmitter and channel noise. The output point is spread out than the input due to adding the noise and the spurious signal level.

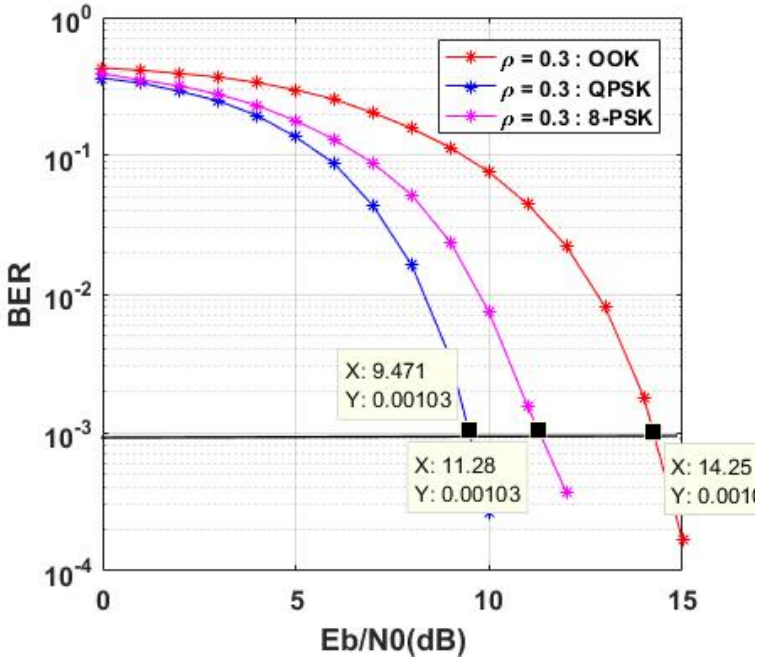

Figure 4.11: BER vs SNR of the OOK, QPSK and 8-PSK modulation schemes at $\rho = 0.3$.

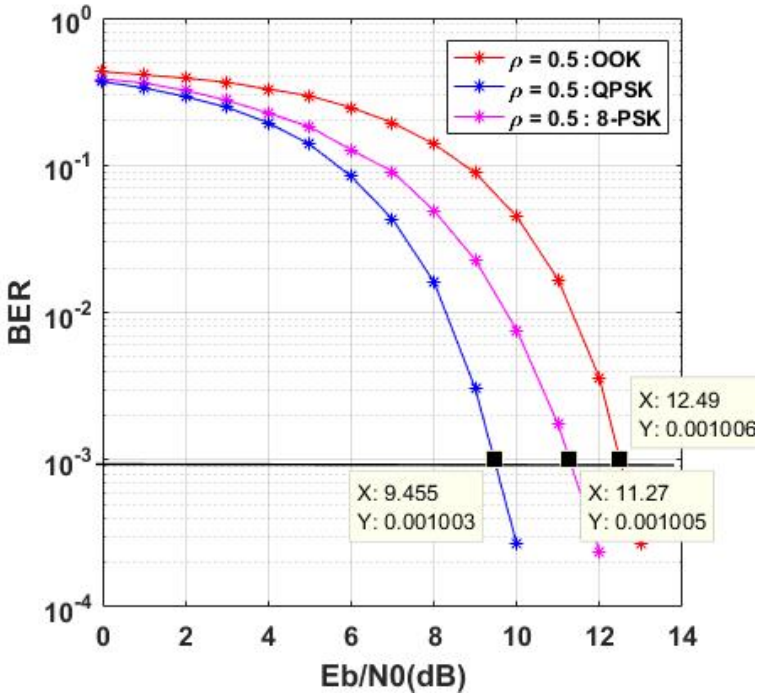

Figure 4.12: BER vs SNR of the OOK, QPSK and 8-PSK modulation schemes at $\rho = 0.5$.

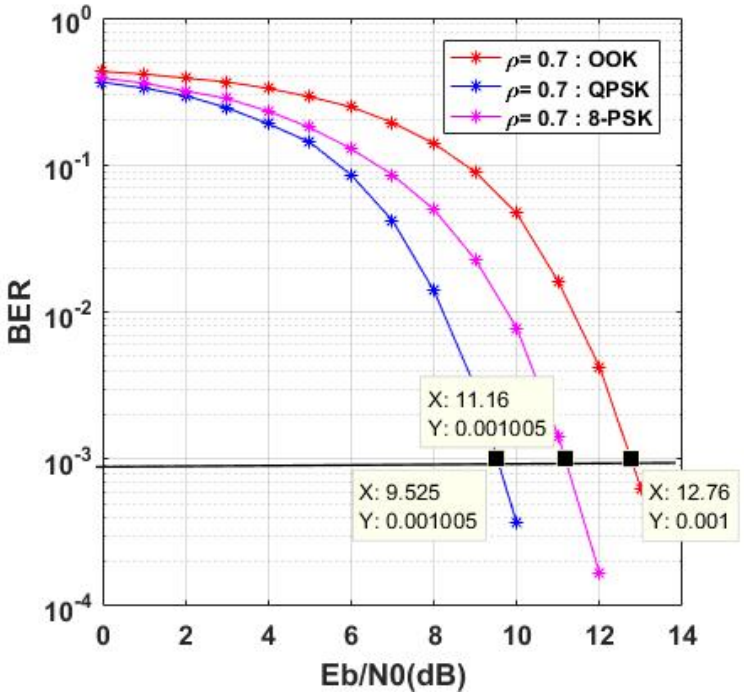

Figure 4.13: BER vs SNR of the OOK, QPSK and 8-PSK modulation schemes at $\rho = 0.7$.

Figure 4.11 shows the BER vs SNR of the OOK modulation scheme, Figure 4.12 shows the BER vs SNR of the QPSK modulation scheme and Figure 4.13 shows the BER vs SNR of the 8-PSK modulation scheme. It consider the different power splitting factors (ρ) such as 0.7, 0.5 and 0.3. The QPSK shows the outperform the 8-PSK and OOK. The QPSK can transmit 2 bits per second and M=4. The 8-PSK can transmit 3 bits per second and M=8. When compare the QPSK and 8-PSK, 8-PSK is more susceptible to noise as the symbols get closer together. Therefore, QPSK outperforms 8-PSK. Moreover, OOK is shown the worst performance due to OOK being susceptible to noise as the bits get closer together than QPSK and 8-PSK.

4.1.3 Behaviour of the ID Data Rate Vs Splitting Coefficient in PS and TS SLIPT Architectures

In this section, we observe the behaviour of SLIPT architectures and in Section 3.2.2 explained the mathematical background of the ID data rate.

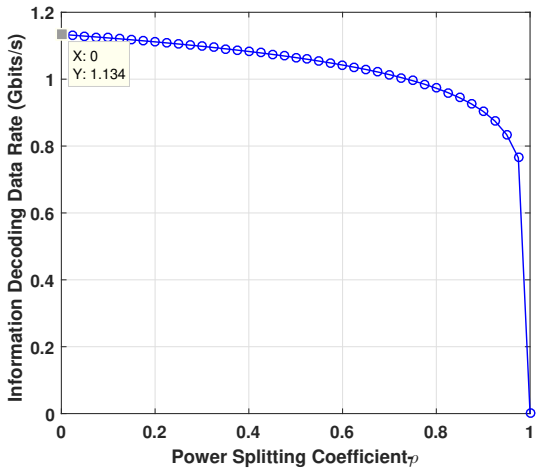

Figure 4.14: Information decoding data rate vs power splitting coefficient.

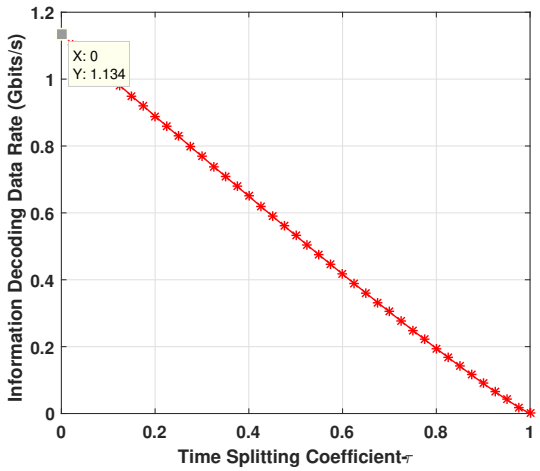

Figure 4.15: Information decoding data rate vs time splitting coefficient.

In Figure 4.14 and Figure 4.15, we plot the ID data rate of TS and PS architectures with splitting coefficient τ and ρ. Since we have maximum ID data rate at τ=0 and ρ=0 due to maximum allocated time and maximum allocated power given at '0' value according to the (1-τ) and (1-ρ) ratio used for the ID process. When reaching the splitting coefficient is 0.975 speedily decreased the ID data rate in PS SLIPT architecture. Moreover, we notice that the PS SLIPT architecture obtain a higher data rate than the TS SLIPT architecture.

4.1.4 Observe the Behaviour of the EH Vs Splitting Coefficient in PS and TS SLIPT Architectures

In this section, we analyze the amount of harvested energy of SLIPT architectures and in Section 3.2.3 explain the mathematical background of the EH.

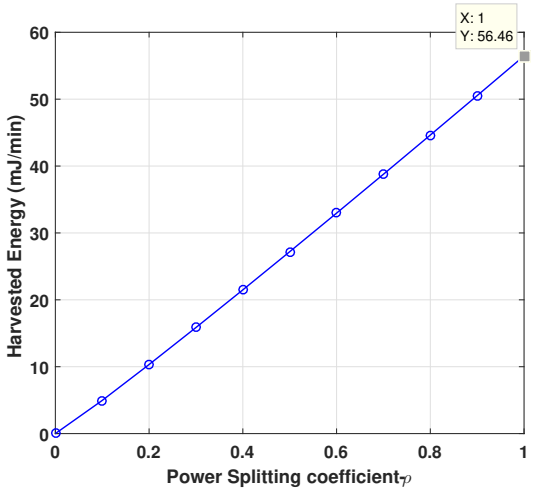

Figure 4.16: The amount of harvested energy vs power splitting coefficient.

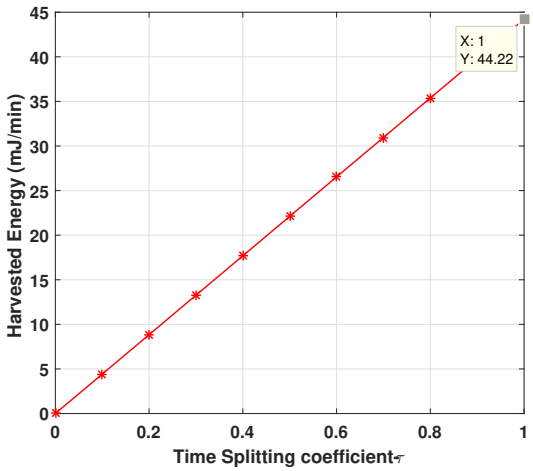

Figure 4.17: The amount of harvested energy vs time splitting coefficient.

Energy harvesting performance of the PS and TS LOS-based SLIPT is also shown in Figure 4.16 and Figure 4.17 respectively. It observe that the amount of EH has increase while increase the splitting coefficient ρ and τ. In PS SLIPT architecture can achieve maximum harvested energy 56.46mJ per min and the same condition the TS SLIPT architecture can achieve maximum harvested energy is 44.22mJ per min. Hence, we can emphasize PS SLIPT receiver architecture harvested more energy in the same condition.

4.1.5 Observe the Behaviour of the EH vs ID in PS and TS SLIPT Architectures for Different Bias Values

In this section, we observe the behaviour of SLIPT architectures with DC bias effect and amplitude of the information signal and in Section 3.2.2 and 3.2.3 explain the mathematical background of the system model.

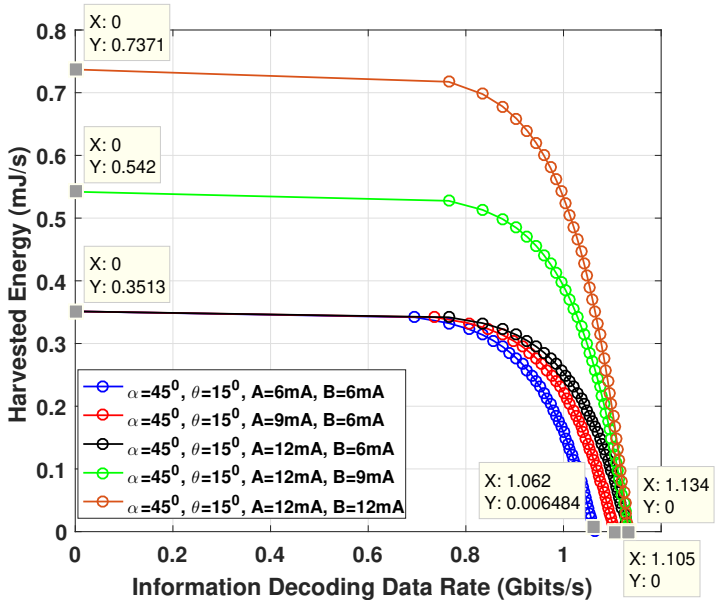

Figure 4.18: The amount of harvested energy vs information decoding data rate in PS SLIPT architecture.

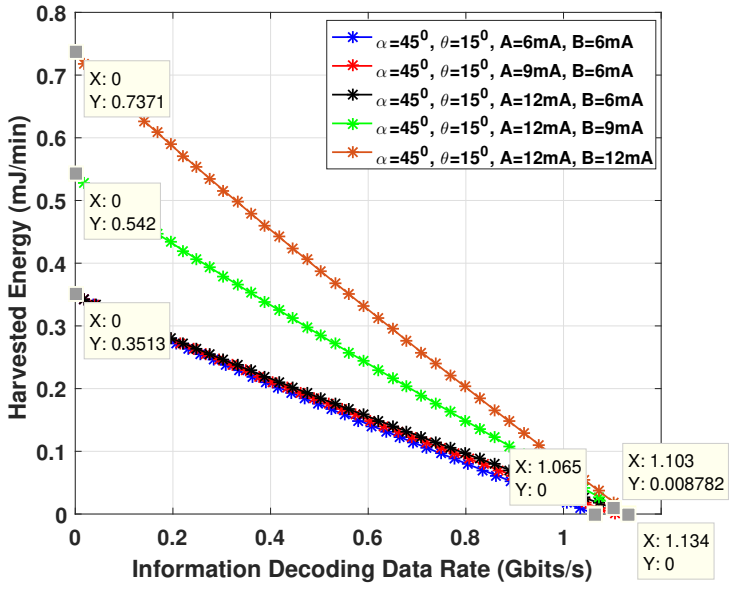

Figure 4.19: The amount of harvested energy vs information decoding data rate in PS SLIPT architecture.

The amount of harvested energy vs information decoding data rate in PS and TS SLIPT architectures is shown in Figure 4.18 and Figure 4.19 respectively. Here, we consider only direct LED with LoS. Further, the FoV of LED (α) is the constant value is 45^0 and used the value of FoV for solar cells is 15^0. Moreover, we consider B=12mA, 9mA and 6mA with the effect of the different values of the bias signal. we can observe the significant difference between each output waveform for both systems. As we notice the maximum amount of harvested energy given at B is 12mA in both systems. When increasing the bias signal (B), harvested energy also increases in both systems. However, when considering both systems, the PS SLPT receiver architecture performs superior to TS SLIPT receiver architecture.

4.1.6 The Sub Optimal Splitting Coefficient with BER in PS and TS SLIPT Architectures Under AWGN

In this section, we observe the sub optimal splitting coefficient of SLIPT architectures and in Section 3.2.1 and 3.2.2 explain the mathematical background of the proposed system.

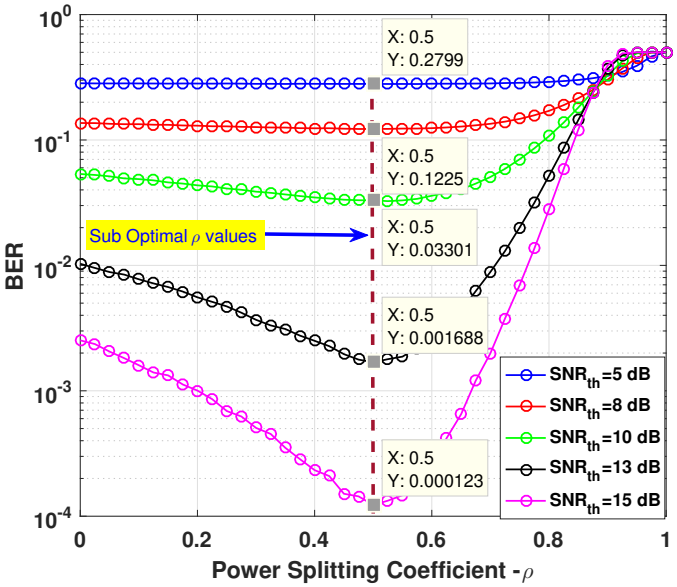

Figure 4.20: The sub optimal values of the ρ which given the minimum BER at SNR_{th} values are 5 dB, 8 dB, 10 dB, 13 dB and 15 dB of the PS SLIPT architecture.

Figure 4.20 shows the sub-optimal values of the different SNR_{th} values are 5 dB, 8 dB, 10 dB, 13 dB and 15 dB. It is considered the minimum BER has given

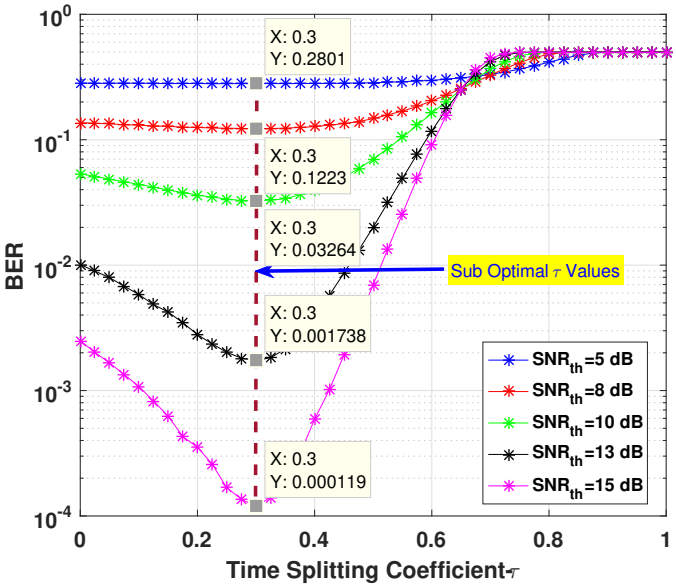

Figure 4.21: The sub optimal values of the τ which given the minimum BER at SNR_{th} values are 5 dB, 8 dB, 10 dB, 13 dB and 15 dB of the TS SLIPT architecture.

PS coefficient. When increasing the SNR the BER is decreased. However, when increasing the SNR the PS coefficient doesn't have change. It is approximately ρ is 0.5 .

Figure 4.21 shows the sub-optimal values of the different SNR_{th} values are 5 dB, 8 dB, 10 dB, 13 dB and 15 dB. It consider the minimum BER has given TS coefficient. When increasing the SNR the BER decrease. However, when increasing the SNR the TS coefficient doesn't have change. It is approximately τ is 0.3.

4.1.7 Calculate the Amount of Harvested Energy for Optimal Splitting Coefficient and Assume Threshold SNR

SNR_{th}	PS Coefficient		TS Coefficient		PS Harvested Energy (mJ/min)	TS Harvested Energy (mJ/min)	BER	
	ID	EH	ID	EH			PS	TS
5	0.5	0.5	0.7	0.3	27.2	22.11	0.2799	0.2801
8	0.5	0.5	0.7	0.3	27.2	22.11	0.1225	0.1223
10	0.5	0.5	0.7	0.3	27.2	22.11	0.033	0.0326
13	0.5	0.5	0.7	0.3	27.2	22.11	0.0017	0.00174
15	0.5	0.5	0.7	0.3	27.2	22.11	0.00012	0.00012

Table 4.2: Amount of harvested energy and the BER values in the PS and TS SLIPT architectures.

Table 4.2 shows the comparison of the PS SLIPT system and TS SLIPT system with the numerical values of the results. Also, consider the amount of harvested energy, BER, SNR threshold values and the sub-optimal values of the splitting coefficient. According to the values, the PS SLIPT system harvested more energy than the TS SLIPT systems.

4.1.8 Analyze the PS and TS SLIPT Architecture in EH and ID

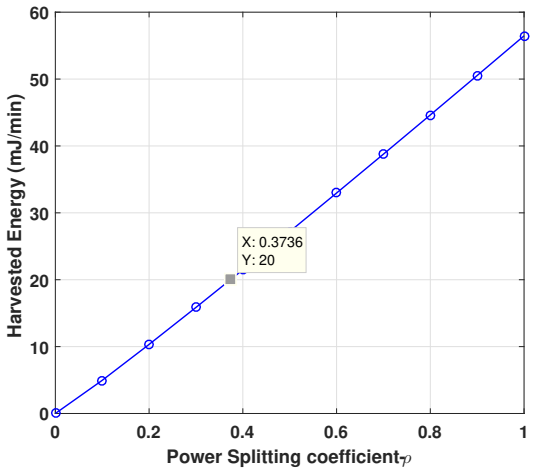

Figure 4.22: Harvested energy vs PS splitting factor for harvest 20 mJ/min.

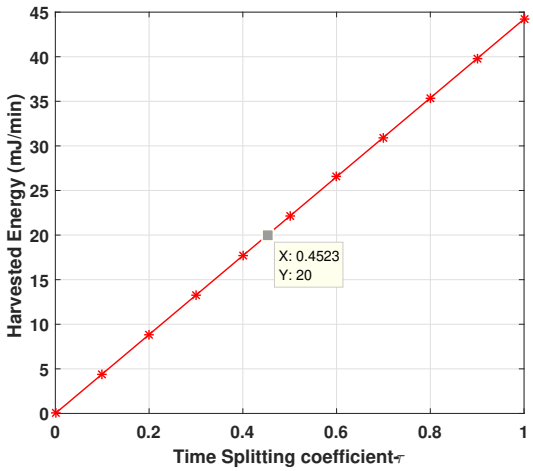

Figure 4.23: Harvested energy vs TS splitting factor for harvest 20 mJ/min.

Figure 4.22 shows the PS splitting coefficient to the amount of harvested energy 20mJ per minute. The PS splitting coefficient is 0.3736. Figure 4.23 shows the TS splitting coefficient to the amount of harvested energy 20mJ per

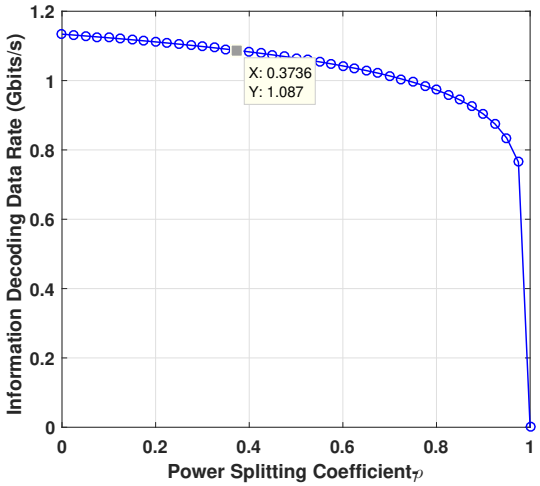

Figure 4.24: Information decoding data rate vs PS splitting factor is 0.3736 for harvest 20 mJ/min.

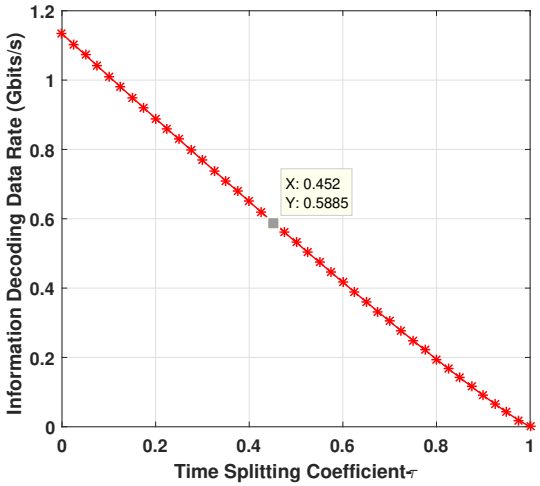

Figure 4.25: Information decoding data rate vs TS splitting factor is 0.4523 for harvest 20 mJ/min.

minute. The TS splitting coefficient is 0.4523. Figure 4.24 shows the information decoding data rate for the splitting coefficient is 0.3736 in PS SLIPT architecture. Figure 4.24 shows the information decoding data rate is 1.087 Gbits per second for the splitting coefficient is 0.3736 in PS SLIPT architecture and Figure 4.25 shows the information decoding data rate is 0.588 Gbits per second for the splitting coefficient is 0.4523 in TS SLIPT architecture.

4.2 A SLIPT-assisted Visible Light Communication Scheme

In this section, we discuss the two schemes such as SLIPT and SWIPT. For the SLIPT scheme, we use PS SLIPT receiver architecture. Further, we analyze the BER, the outage probability and the amount of harvested energy of the SLIPT & SWIPT system.

4.2.1 BER Analysis of the SWIPT and SLIPT

In this Section, we present the numerical and simulation results of the SLIPT and SWIPT system models and in section 3.3.1 explain the theoretical & mathematical background.

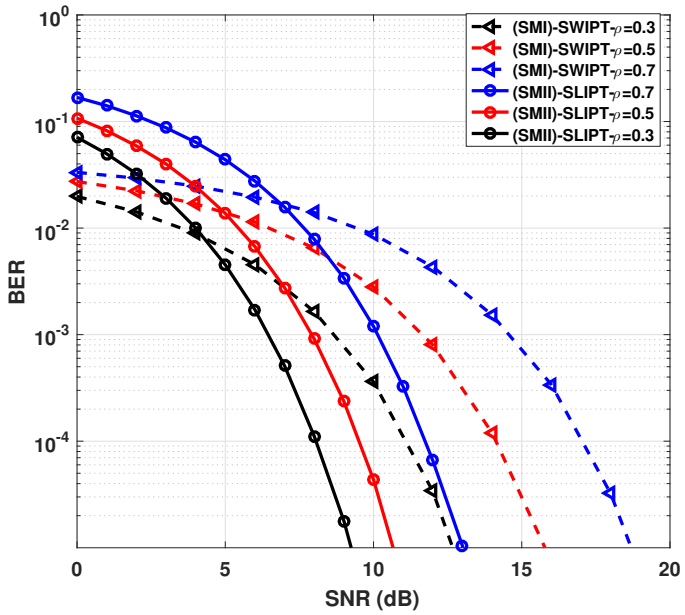

Figure 4.26: BER performance of the indoor wireless system using LOS-based SLIPT scheme

In SM-I, the BER and outage probability investigate for different values of SNR, signal transmission power P_t, different time slots t and energy harvesting coefficient α. Unless otherwise stated, in all simulations, we use the fixed values for $\eta_e = 0.5$, the signal transmission power $P_t = 30dBm$. Moreover, the distance between source and transmitter used for simulation $d = 10m$. The reliability of the proposed indoor wireless system is observed by analyzing the BER performance of the SM-I against the SNR values for $(t, \alpha) \in (0.3, 0.5, 0.7)$ as shown in Figure 4.26. Since,the decreasing α would increase the 1- α, it can be seen that the decrements of α values with the same SNR condition the BER performance

is significantly improve. As it can be observed by Figure 4.26, the decreasing α values will increase the BER performance. So it is obvious that, power splitting factor α directly affected to BER and choosing an optimum value for α is required for a quality received signal. In Figure 4.26, depict the more detailed comparison of BER performance SM-I and SM-II. SLIPT and SWIPT scheme performances on the same SNR condition and degradation are summarized by simulation results as in Figure 4.26.

4.2.2 Outage Probability Analysis of the SWIPT and SLIPT

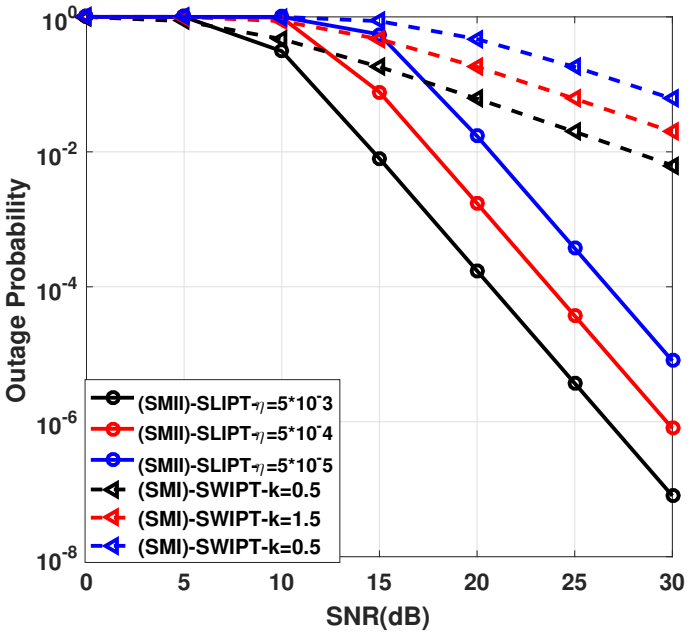

Figure 4.27: Outage performance of both SM-I and SM-II for indoor wireless system using LOS-based SLIPT scheme at the fixed data rate R=1 $b/s/Hz$.

The outage probability of the proposed indoor wireless system using LOS-based SLIPT scheme is shown in Figure 4.27 for the minimum achievable data rate of R_{min}=1$b/s/Hz$. The performance of the proposed system is compared with the SWIPT based wireless system. Numerical parameters considered for SLIPT system are: dimming factor ϵ=0.5, shot noise variance, σ_{sh}^2=10^{-7} W/Hz, thermal noise variance σ_{th}^2=10^{-7} W/Hz, system bandwidth W=$2\times10^6 Hz$, power splitter $\alpha = 0.5$. The following numerical parameters are used in SWIPT system: distance between source and destination $d = 10m$, power splitting coefficient $\alpha = 0.5$. It is observed that the outage performance of the proposed SLIPT based indoor system is significantly improved by increasing the photo detector responsivity. Also it is

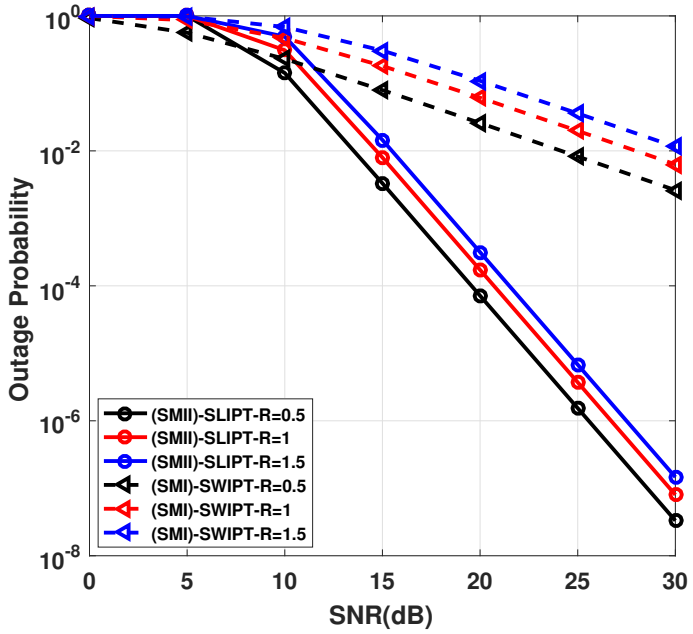

Figure 4.28: Outage performance of the SLIPT based indoor wireless system for the various data rates.

noted that since the SLIPT based indoor wireless system working with minimum path loss rather than SWIPT system, the proposed system is outperform when comparing with the system operating with SWIPT scheme. Further, it is observed that the SM-II with detector responsivity of η=5$\times$ 10^{-3} require 15dB SNR to achieve the target outage of 10^{-2} whereas the SM-I requires around 28dB SNR when k=0.5.

In Figure 4.28, the outage probability of the SM-I SWIPT and SM-II SLIPT are shown for the various achievable data rates. For simulating the outage probability of the SWIPT system, the following numerical parameters are used: $k = 0.5$, $\alpha = 0.5$ and $d = 10m$. Also, in Figure 4.28, to simulate the SLIPT system the following numerical parameters are used: $\alpha = 0.5$, $d = 1m$, $\epsilon = 0.5$ and $\eta = 5 \times 10^{-3}$. It observe that the outage performance of the proposed indoor wireless system increase by reducing the achievable data rate from $1b/s/Hz$ to 0.5 $b/s/Hz$. Additionally, it is noted that for the target outage of 10^{-2} and for the minimum targeted data rate of 0.5 $b/s/Hz$, the proposed SM-II wireless system require 14dB SNR, whereas the indoor wireless system operating with SM-I require 24dB SNR.

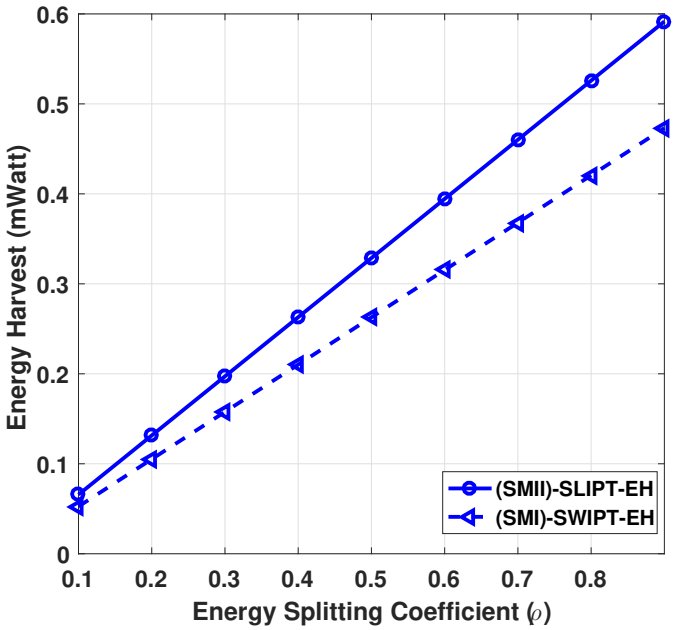

Figure 4.29: Energy harvesting of the proposed SLIPT based indoor wireless system versus power splitting factor ρ.

4.2.3 Amount of Harvested Energy in SWIPT and SLIPT

Energy harvesting performance of the proposed indoor wireless system using LOS-based SLIPT is also shown in Figure 4.29. It is observed that the amount of EH has increased while increasing the power split coefficient α. It should be emphasized that at α= 0.5, the proposed SLIPT receiver harvest the power of 0.32 mW, whereas the system working with SWIPT scheme harvest 0.28 mW. Since, the SM-II system has very low noise variance and path loss when compare with SM-I, it achieves better performance than SM-I.

4.3 Chapter Summary

In this chapter, we consider the simulation and numerical results of the proposed system models. There are two basic parts of the results and discussion. In the first part first section, we compare and observe the FoV of Tx and Rx to achieve maximum receive power in the VLC system. The Tx FoV is 45 and RX FoV is 15. The second section analyzes the BER of the PS SLIPT architecture with three different modulation schemes such OOK, QPSK and 8-PSK. According to the results, QPSK outperforms 8-PSK and OOK. In the third section, we compare the behaviour of the ID data rate vs splitting coefficient of the TS SLIPT architecture

and PS SLIPT architecture. In both architectures have two different behaviours and PS SLIPT architecture outperform TS SLIPT architecture. In the fourth section, we compare the amount of harvested energy of both architectures. With the results, the PS SLIPT system harvested more energy than the TS SLIPT system. Also, in the fifth section, we consider the amount of harvested energy vs ID data rate of both architectures.

In the second part first section, we analyze the BER of the SWIPT and SLIPT. With the simulation results, the splitting coefficient directly affected the BER and SLIPT system shows a low BER than SWIPT when SNR is low. In the second section, we compare the outage probability of both systems. The SLIPT system shows good performance than the SWIPT system model. In the last section, we observe the amount of harvested energy of the SLIPT and SWIPT system. The SLIPT system harvests more energy than the SWIPT system.

Chapter 5

CONCLUSIONS AND FUTURE DIRECTIONS

5.0.1 CONCLUSIONS

This chapter concludes the work of performance analysis of the PS-SLIPT architecture. Also, present the new findings and contributions of the research. This thesis has concentrated on the PS-SLIPT system model and discussed the comprehensive analysis of the VLC and RF. In addition, discussed the benefits of VLC over RF and the trending applications of VLC. Further, studied the VLC system model and main parts of the communication system such as transmitter, receiver and channel. In the transmitter, studied the LED and the important parameters of the LED. In addition, studied the modulation schemes of the transmitter. In the receiver, studied the PD and important parameters of the PD. Moreover, we considered the channel model in VLC and configurations.

We considered the indoor communication system model and select the LoS free space channel. We explained the mathematical model of the VLC transmitter, receiver and LoS free space channel. Further, we used the Lambartian system model. Moreover, according to the simulation, we selected the optimum FoV of the transmitter and the receiver. The optimum FoV gave the maximum receiver power in the VLC system model.

The next contribution is to compared the SLIPT receiver architectures. It is TS-SLIPT and PS-SLIPT receiver architectures. We compared the modulation schemes in the PS-SLIPT system model such as OOK, QPSK and 8-PSK. Further, we observed the performance of PS-SLIPT and TS–SLIPT receiver architectures under BER, SNR, information data rate and harvested energy. According to the numerical and simulation results, PS-SLIPT receiver architecture performed better than TS-SLIPT architecture under the ID and EH simultaneous functions.

In the last stage, we compared SLIPT and SWIPT system models in indoor communication. The SLIPT and SWIPT system used PS-SLIPT receiver architecture. We compared BER, SNR, outage probability and amount of harvested energy of both systems. The SLIPT system model outperforms the SWIPT sys-

tem model.

5.0.2 FUTURE DIRECTIONS

In SLIPT systems need simultaneous ID and EH. Therefore, robustness is an important factor to be considered in the communication channel. The next future direction is to decrease the noises affected by the SLIPT system. Also, suggest the technology to reduce the ambient noise for the VLC channel [3]. The next future direction is to increase the communication distance using LoS and non-LoS. Reflection and obstacles are reasons for the quality degradation of the ID signal and it is directly affected the range of the communication. Efficiently enhancing the SNR is another future direction of the SLIPT system. To maintain the quality of the signal enhance the SNR and maintain the LoS using the proper method [77]. The next important suggestion is to increase the data rate. During many research proved VLC able to achieve Gb/s data rates. Using proper modulation techniques and optimizing the parameters can be achieved a high data rate for the SLIPT system. The MIMO is the last future direction to apply the SLIPT system. In indoor communication, MIMO is more practical due to various lights used within the room [78].

There are several issues emphasized to overcome in hybrid communication. Such as network selection, access protocol, heterogeneous receiver type, handover, load balancing, high-capacity backhaul network, seamless steering of transmitted data, modulation techniques in optical/optical wireless hybrid systems and performance enhancement in mixed RF/FSO relay systems. Future researchers can overcome these issues in the hybrid communications system model [22]. When we use the RAT communication system, it is important to select the place for the relay location. Also, when we use the AF method noises are amplified. It is corrupt the original signal and it is harmful to the information signal [23].

There are a few future directions for the researchers in the FSO apply for the DCN such as available optical modulators work in IR range and DCN-FSO work in the visible range, artificial light source, misalignment due to the vibration of server fans and UPS [25].

There are a few future directions discuss relate to EH in VLC. First, we focus on the RF/VLC hybrid systems. To achieve the limit of power consumption the RF/VLC hybrid system is properly synchronous with each other [77]. To improve the performance of the RF/VLC hybrid system, present the new optimization techniques. Also, introduce the properly optimised network to implement the hybrid system and power-efficient systems. Due to health conditions, wifi can

remove and apply VLC ystem in the indoor network. Suggest the novel applications to implement the RF/VLC hybrid system [79].

References

[1] A. Aldalbahi, M. Rahaim, A. Khreishah, M. Ayyash, and T. D. C. Little, "Visible light communication module: An open source extension to the ns3 network simulator with real system validation," *IEEE Access*, vol. 5, p. 22144–22158, 2017.

[2] G. Pan, P. D. Diamantoulakis, Z. Ma, Z. Ding, and G. K. Karagiannidis, "Simultaneous lightwave information and power transfer: Policies, techniques, and future directions," *IEEE Access*, vol. 7, p. 28250–28257, 2019.

[3] A. T. Hussein, "Visible light communication system," *PhD thesis, School of Electronic and Electrical Engineering, University of Leeds*, 2016.

[4] E. Udvary, "Visible light communication survey," *Infocommunications journal*, no. 2, p. 22–31, 2019.

[5] T. Cevik and S. Yilmaz, "An overview of visible light communication systems," *International journal of Computer Networks Communications*, vol. 7, no. 6, p. 139–150, 2015.

[6] S. Rehman, S. Ullah, P. Chong, S. Yongchareon, and D. Komosny, "Visible light communication: A system perspective—overview and challenges," *Sensors*, vol. 19, no. 5, p. 1153, 2019.

[7] M. Z. Chowdhury, M. T. Hossan, A. Islam, and Y. M. Jang, "A comparative survey of optical wireless technologies: Architectures and applications," *IEEE Access*, vol. 6, p. 9819–9840, 2018.

[8] Z. Ghassemlooy, *Visible light communications: theory and applications*. CRC Press, 2019.

[9] M. A. Khalighi and M. Uysal, "Survey on free space optical communication: A communication theory perspective," *IEEE Communications Surveys Tutorials*, vol. 16, no. 4, pp. 2231–2258, 2014.

[10] M. Z. Chowdhury, M. T. Hossan, A. Islam, and Y. M. Jang, "A comparative survey of optical wireless technologies: Architectures and applications," *IEEE Access*, vol. 6, p. 9819–9840, 2018.

[11] X. Chen, C. Min, and J. Guo, "Visible light communication system using silicon photocell for energy gathering and data receiving," *International Journal of Optics*, vol. 2017, p. 1–5, 2017.

[12] T. D. P. Perera, D. N. K. Jayakody, S. Affes, M. Chidambaranathan, and C. Yury, "Wireless-powered hybrid terrestrial and underwater cooperative communication system," *2019 15th International Conference on Distributed Computing in Sensor Systems (DCOSS)*, 2019.

[13] P. D. Diamantoulakis, K. N. Pappi, Z. Ma, X. Lei, P. C. Sofotasios, and G. K. Karagiannidis, "Airborne radio access networks with simultaneous lightwave information and power transfer (slipt)," *2018 IEEE Global Communications Conference (GLOBECOM)*, 2018.

[14] H. G. Sandalidis, A. Vavoulas, T. A. Tsiftsis, and N. Vaiopoulos, "Illumination, data transmission, and energy harvesting: the threefold advantage of vlc," *Applied Optics*, vol. 56, no. 12, p. 3421, 2017.

[15] M. Ali, T. Perera, S. S. Morapitiya, D. N. Jayakody, S. Panic, and S. Garg, *A Hybrid RF/FSO and Underwater VLC Cooperative Relay Communication System,*. 14th International Forum On Strategic Technology-IFOST, 2019.

[16] J. R. Barry, "Wireless infrared communications," 1994.

[17] T. D. P. Perera, D. N. K. Jayakody, S. K. Sharma, S. Chatzinotas, and J. Li, "Simultaneous wireless information and power transfer (swipt): Recent advances and future challenges," *IEEE Communications Surveys Tutorials*, vol. 20, no. 1, p. 264–302, 2018.

[18] G. Pan, H. Lei, Z. Ding, and Q. Ni, "On 3-d hybrid vlc-rf systems with light energy harvesting and oma scheme over rf links," *GLOBECOM 2017 - 2017 IEEE Global Communications Conference*, 2017.

[19] A. M. Abdelhady, O. Amin, A. Chaaban, and M.-S. Alouini, "Resource allocation for outdoor visible light communications with energy harvesting capabilities," *2017 IEEE Globecom Workshops (GC Wkshps)*, 2017.

[20] P. D. Diamantoulakis, G. K. Karagiannidis, and Z. Ding, "Simultaneous lightwave information and power transfer (slipt)," *IEEE Transactions on Green Communications and Networking*, vol. 2, no. 3, 2018.

[21] A. Rauniyar, P. E. Engelstad, and O. N. Osterbo, "On the performance of bidirectional noma-swipt enabled iot relay networks," *IEEE Sensors Journal*, vol. 21, no. 2, p. 2299–2315, 2021.

[22] M. Z. Chowdhury, M. K. Hasan, M. Shahjalal, M. T. Hossan, and Y. M. Jang, "Optical wireless hybrid networks: Trends, opportunities, challenges, and research directions," *IEEE Communications Surveys Tutorials*, vol. 22, no. 2, pp. 930–966, 2020.

[23] W. Liu, J. Ding, J. Zheng, X. Chen, and C.-L. I, "Relay-assisted technology in optical wireless communications: A survey," *IEEE Access*, vol. 8, pp. 194 384–194 409, 2020.

[24] M. A. Khalighi and M. Uysal, "Survey on free space optical communication: A communication theory perspective," *IEEE Communications Surveys & Tutorials*, vol. 16, no. 4, pp. 2231–2258, 2014.

[25] A. S. Hamza, J. S. Deogun, and D. R. Alexander, "Wireless communication in data centers: A survey," *IEEE Communications Surveys & Tutorials*, vol. 18, no. 3, pp. 1572–1595, 2016.

[26] J. S. A. Hamza, Abdelbaset S. Deogun and D. R., "Classification framework for free space optical communication links and systems," *IEEE Communications Surveys & Tutorials*, vol. 21, no. 2, pp. 1346–1382, 2019.

[27] V. Manea, S. Puscoci, and D. A. Stoichescu, "Considerations on interference between fso systems," *2018 10th International Conference on Electronics, Computers and Artificial Intelligence (ECAI)*, 2018.

[28] D. Pauluzzi, P. Mcconnell, and R. Poulin, "Free-space, undirected infrared (ir) voice and data communications with a comparison to rf systems," *1992 IEEE International Conference on Selected Topics in Wireless Communications.*

[29] S. Kaur and A. Kakati, "Analysis of free space optics link performance considering the effect of different weather conditions and modulation formats

for terrestrial communication," *Journal of Optical Communications*, vol. 41, no. 4, p. 463–468, 2020.

[30] N. Dahiya, A. Ahmed, and S. Kaur, "Optimization of free space optical terrestrial link considering different system parameters," *2020 8th International Conference on Reliability, Infocom Technologies and Optimization (Trends and Future Directions) (ICRITO)*, 2020.

[31] "Li-fi: Light fidelity-the transmission of data through light," *International Journal of Science and Research (IJSR)*, vol. 6, no. 7, p. 196–200, 2017.

[32] L. U. Khan, "Visible light communication: Applications, architecture, standardization and research challenges," *Digital Communications and Networks*, vol. 3, no. 2, p. 78–88, 2017.

[33] L. E. M. Matheus, A. B. Vieira, L. F. M. Vieira, M. A. M. Vieira, and O. Gnawali, "Visible light communication: Concepts, applications and challenges," *IEEE Communications Surveys Tutorials*, vol. 21, no. 4, p. 3204–3237, 2019.

[34] E. Udvary, "Visible light communication survey," *Infocommunications journal*, no. 2, p. 22–31, 2019.

[35] N. Chi, "Visible light communication receiving technology," *LED-Based Visible Light Communications Signals and Communication Technology*, p. 59–90, 2018.

[36] Z. Song and S. Peng, "A simple implementation of long distance visible light communication system," *Management Information and Optoelectronic Engineering*, pp. 349–355, 2017.

[37] K. S. Thai-Chien Bui, Suwit Kiravittaya and N.-H. Nguyen, "A comprehensive lighting configuration for efficient indoor visible light communication networks," *International Journal of Optics*, 2016.

[38] M. S. a. S. M.V. Bhalerao1, "Line of sight model for visible light communication using lambertian radiation pattern of led," *International Journal of Communication Systems*, December 2016.

[39] D. R. B. Dragomir Radu and P. Brandusa, "Irradiance scenario of a non-lambertian intensity led assembly," *Electrical and Power Engineering - EPE*, 2014.

[40] H. L. M. S. R. M. D. Wu, Z. Ghassemlooy and X. Tang, "Optimisation of lambertian order for indoor non-directed optical wireless communication," *2012 1st IEEE International Conference on Communications in China Workshops (ICCC)*, pp. 43–48, 2012.

[41] S. Mr.B.Vinodhkumar, "Implementation of vlc transceiver for audio and video signal using li-fi technology," *IOSR Journal of Engineering (IOSR JEN)*, pp. 27–30, 2019.

[42] G. B. Fatemeh Madani and Z. Ghassemlooy, "Effect of transmitter and receiver parameters on the output signal to noise ratio in visible light communications," *25th Iranian Conference on Electrical Engineering (ICEE2017)*, 2017.

[43] M. M. J. Faisal A. Dahri, Sajjad Ali, "A review of modulation schemes for visible light communication," *IJCSNS International Journal of Computer Science and Network Security*, vol. VOL.18 No.2, 2018.

[44] U. S. M. Amgad F. Aziz, Omar A. M. Aly and, "High efficiency modulation technique for visible light communication (vlc)," *36th NATIONAL RADIO SCIENCE CONFERENCE (NRSC 2019)*, 2019.

[45] T.-C. Bui and S. Kiravittaya, "High efficient modulation techniques for indoor visible light communication," *International Journal of Optics*, 2016.

[46] X. G. N Bamiedakis and I. H. White, "Wireless visible light communications employing feed-forward pre-equalization and pam-4 modulation," *Journal of Lightwave Technology*, 2016.

[47] F. J. A. M. Zaiton, H. R. A. Rahim, "Performance characterization of phase shift keying modulation techniques for indoor visible light communication system," *The 2nd International Conference on Applied Photonics and Electronics (InCAPE 2019)*, 2019.

[48] Z. G. M. U. A. C. Boucouvalas, Periklis Chatzimisios and K. Yiannopoulos, "Standards for indoor optical wireless communications," *IEEE Communications Magazine*, 2015.

[49] X. B. . J.-Y. W. Sheng-Hong Lin, Cheng Liu, "Indoor visible light communications: performance evaluation and optimization," *EURASIP Journal on Wireless Communications and Networking volume*, 2018.

[50] I. U. Edward Fisher and R. Henderson, "A reconfigurable single-photon-counting integrating receiver for optical communications," *IEEE JOURNAL OF SOLID-STATE CIRCUITS*, vol. VOL. 48, NO. 7, 2013.

[51] T. A. Syifaul Fuada, Angga Pratama Putra, "Analysis of received power characteristics of commercial photodiodes in indoor los channel visible light communication," *(IJACSA) International Journal of Advanced Computer Science and Applications*, vol. Vol. 8, No. 7, 2017.

[52] M. Irshad and M. M. Bilal, "An indoor los non-los propagation analysis using visible light communication," *International Journal of Advanced Research in Computer Engineering Technology (IJARCET)*, vol. Volume 7, Issue 10, October 2018.

[53] H.-H. C. Yang Qiu and W.-X. Meng, "Channel modeling for visible light communications—a survey," *WIRELESS COMMUNICATIONS AND MOBILE COMPUTING*, October 2016.

[54] L. H. Yuan Zhuang and H. Haas, "A survey of positioning systems using visible led lights," *IEEE COMMUNICATIONS SURVEYS TUTORIALS*, vol. VOL. 20, NO. 3, THIRD QUARTER 2018.

[55] R. M. N. Mohammad Asif Hossain and S. S. Anjum, "A survey on simultaneous wireless information and power transfer with cooperative relay and future challenges," 2019.

[56] L. W. R. M. Jinglan Ou, Hangchuan Shi and H. Wu, "Analysis of swipt-enabled relay networks with full-duplex destination-aided jamming," 2021.

[57] a. J. G. Xiongbin Chen, ChengyuMin, "Visible light communication system using silicon photocell for energy gathering and data receiving," *International Journal of Optics*, vol. Volume 2017, Article ID 6207123, 5 pages, 2017.

[58] A. C. Amr M. Abdelhady, Osama Amin and M.-S. Alouini, "Resource allocation for outdoor visible light communications with energy harvesting capabilities," *IEEE Proceedings*, 2017.

[59] P. D. Diamantoulakis and G. K. Karagiannidis, "Simultaneous lightwave information and power transfer (slipt) for indoor iot applications," *GLOBECOM 2017 - 2017 IEEE Global Communications Conference*, 2017.

[60] H. L. Z. D. Gaofeng Pan, y and Q. Niy, "On 3-d hybrid vlc-rf systems with light energy harvesting and oma scheme over rf links," *IEEE Proceedings*, 2017.

[61] H. L. Gaofeng Pan and Z. Ding, "3-d hybrid vlc-rf indoor iot systems with light energy harvesting," *IEEE Transactions on Green Communications and Networking*, 2018.

[62] M. J. M. D. Mateo Marceli´c, Branimir Iv˘si´c, "Estimation of energy harvesting capabilities for rf and other environmental sources," *IEEE Proceedings*, 2018.

[63] H. L. F. Z. Y. W. Shuai Ma, Fan Zhang and S. Li, "Simultaneous lightwave information and power transfer in visible light communication systems," *IEEE Transactions on Wireless Communications*, 2019.

[64] Z. M. Z. D. GAOFENG PAN, PANAGIOTIS D. DIAMANTOULAKIS and G. K. KARAGIANNIDIS, "Simultaneous lightwave information and power transfer: Policies, techniques, and future directions," *IEEE access*, 2019.

[65] Krikidis, "Simultaneous wireless information and power transfer in modern communication systems," *IEEE COMMUNICATIONS SURVEYS TUTORIALS*, 2014.

[66] D. N. D. I. K. X. Lu, P. Wang and Z. Han, "Wireless networks with rf energy harvesting: A contemporary survey," *IEEE COMMUNICATIONS SURVEYS TUTORIALS*, vol. vol. 17, no. 2, pp. 757–789, 2015.

[67] Z. Ding, "Application of smart antenna technologies in simultaneous wireless information and power transfer," *IEEE COMMUNICATIONS SURVEYS TUTORIALS*, vol. vol. 53, no. 4, pp. 86–93, 2015.

[68] S. Ulukus, "Energy harvesting wireless communications: A review of recent advances," *IEEE COMMUNICATIONS SURVEYS TUTORIALS*, vol. vol. 33, no. 3,pp. 360–381,, 2015.

[69] N. Zhao, "Exploiting interference for energy harvesting: A survey, research issues, and challenges," *IEEE Access*, vol. vol. 33, no. 3,pp. 360–381, 2017.

[70] Y. C. M.-L. Ku, W. Li and K. R. Liu, "Advances in energy harvesting communications: Past, present, and future challenges,," *IEEE COMMUNICATIONS SURVEYS TUTORIALS*, 2016.

[71] S. U. O. Ozel, K. Tutuncuoglu and A. Yener, "Fundamental limits of energy harvesting communications," *IEEE COMMUNICATIONS SURVEYS TUTORIALS*, vol. vol. 53, no. 4, pp. 126–132, 2015.

[72] H. J. Visser and R. J. M. Vullers, "Rf energy harvesting and transport for wireless sensor network applications: Principles and requirements„" *IEEE proceedings*, vol. vol. 101, no. 6, pp. 1410–1423, 2013.

[73] F. Akhtar and M. H. Rehmani, "Energy harvesting for self-sustainable wireless body area networks," vol. vol. 19, no. 2, pp. 32–40, 2017.

[74] S. Fuada, A. Pratama, and T. Adiono, "Analysis of received power characteristics of commercial photodiodes in indoor los channel visible light communication," *International Journal of Advanced Computer Science and Applications*, vol. 8, no. 7, 2017.

[75] K. J. R. Liu, A. K. Sadek, W. Su, and A. Kwasinski, "Multi-node cooperative communications," *Cooperative Communications and Networking*, p. 194–237.

[76] T. D. P. Perera, D. N. K. Jayakody, S. Affes, M. Chidambaranathan, and C. Yury, "Wireless-powered hybrid terrestrial and underwater cooperative communication system," *2019 15th International Conference on Distributed Computing in Sensor Systems (DCOSS)*, 2019.

[77] T. M. N. N. Sylvester Aboagye, Ahmed Ibrahim and O. A. Dobre, "Vlc in future heterogeneous networks: Energy–and spectral–efficiency optimization," *IEEE Proceedings*, 2020.

[78] A.-M. Căilean and M. Dimian, "Current challenges for visible light communications usage in vehicle applications: A survey," *IEEE Communications Surveys & Tutorials*, 2016.

[79] M. U. F. I. Z. D. X. E. S. K. A. Q. HISHAM ABUELLA, MOHAMMED ELAMASSIE and S. EKIN, "Hybrid rf/vlc systems: A comprehensive survey on network typologies, performance analyses, applications, and future directions," *IEEE Communications Surveys & Tutorials*, 2017.